

Contents lists available at ScienceDirect

Transportation Research Part C

journal homepage: www.elsevier.com/locate/trc





Resiliency of on-demand multimodal transit systems during a pandemic

Ramon Auad ^{a,b}, Kevin Dalmeijer ^a, Connor Riley ^a, Tejas Santanam ^a, Anthony Trasatti ^a, Pascal Van Hentenryck ^{a,*}, Hanyu Zhang ^a

^a H. Milton Stewart School of Industrial and Systems Engineering, Georgia Institute of Technology, United States of America

ARTICLE INFO

Keywords: COVID-19 Public transit On-demand shuttles Multimodal transit systems

ABSTRACT

During the COVID-19 pandemic, the collapse of the public transit ridership led to significant budget deficits due to dramatic decreases in fare revenues. Additionally, public transit agencies are facing challenges of reduced vehicle capacity due to social distancing requirements, additional costs of cleaning and protective equipment, and increased downtime for vehicle cleaning. Due to these constraints on resources and budgets, many transit agencies have adopted essential service plans with reduced service hours, number of routes, or frequencies. This paper studies the resiliency during a pandemic of On-Demand Multimodal Transit Systems (ODMTS), a new generation of transit systems that combine a network of high-frequency trains and buses with on-demand shuttles to serve the first and last miles and act as feeders to the fixed network. It presents a case study for the city of Atlanta and evaluates ODMTS for multiple scenarios of depressed demand and social distancing representing various stages of the pandemic.

The case study relies on an optimization pipeline that provides an end-to-end ODMTS solution by bringing together methods for demand estimation, network design, fleet sizing, and real-time dispatching. These methods are adapted to work in a multimodal setting and to satisfy practical constraints. In particular, a limit is imposed on the number of passenger transfers, and a new network design model is introduced to avoid the computational burden stemming from this constraint. Real data from the Metropolitan Atlanta Rapid Transit Authority (MARTA) is used to conduct the case study, and the results are evaluated with a high-fidelity simulation. The case study demonstrates how ODMTS provide a resilient solution in terms of cost, convenience, and accessibility for this wide range of scenarios.

1. Introduction

At the start of the COVID-19 pandemic, public transit ridership collapsed across the nation as many individuals stayed at home. Public transit agencies saw their budget deficits build as ridership dropped as much as 85% in some cities, leading to a dramatic drop in fare revenue for 2020 compared to 2019 (Goldbaum and Wright, 2020). In addition, public transit agencies are facing the challenging task of providing safe and accessible travel, especially for essential workers, with reduced vehicle capacities, additional costs for protective equipment or supplies, and increased downtime for cleaning.

With constrained vehicle capacity and large budget deficits, many transit agencies have adopted essential service plans that include cutting routes, service hours, or frequencies in order to provide safer service on other routes with their limited resources.

E-mail address: pascal.vanhentenryck@isye.gatech.edu (P. Van Hentenryck).

b Departamento de Ingeniería Industrial, Universidad Católica del Norte, Chile

^{*} Corresponding author.

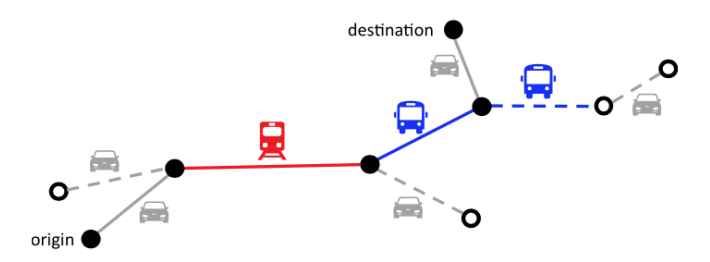


Fig. 1. An ODMTS and an example of a passenger path (solid lines).

New York City's MTA no longer runs 24 h a day (it closes from 1–5am to provide downtime for more effective cleaning) and faces an \$8B deficit (Nessen, 2020). In Boston, the MBTA has tried to preserve as much of the weekday trips as possible for essential workers, but is now looking at dramatic budget cuts due to a deficit of close to \$600M. (Goldbaum and Wright, 2020). At the time of writing, the MBTA is considering cutting their ferry routes and weekend commuter rail services. In Atlanta, the Metropolitan Atlanta Rapid Transit Authority (MARTA) faced similar challenges. In April, MARTA reduced the frequency of the rail network from every 12 min to every 20 min and its essential service plan reduced the number of bus lines from 110 to 41 (Wickert, 2020b). Even as transit planners and operators try to mitigate the effects of these service cuts, many essential workers and community members are still impacted in terms of accessibility and convenience. In Atlanta, many individuals rely on public transit for access to jobs, groceries, education, and healthcare, and are now forced to find alternative forms of transit (Wickert, 2020a). Ridesharing services such as Uber and Lyft are often prohibitively expensive, which makes it crucial that transit services return to normal as soon as possible.

This paper studies the resiliency of On-Demand Multimodal Transit Systems (ODMTS) (Mahéo et al., 2019) during a pandemic. ODMTS is a new generation of transit systems that consist of a network of high-frequency trains and/or buses combined with on-demand shuttles to serve the first and the last miles. In this paper, the *resiliency* of an ODMTS is defined as the measure in which the system is able to provide accessible public transit with a high level of service, within an appropriate budget, when a pandemic results in significantly lower ridership and additional safety requirements. ODMTS can respond to such a decrease in ridership by scaling down the number of on-demand shuttles and/or high-frequency buses. On-demand shuttles keep serving passengers close to where they are, such that access to the system is not compromised. By design, trains and buses are only used to serve busy corridors, which would still see traffic during a pandemic. Fig. 1 illustrates the design of an ODMTS and how it operates. This ODMTS features fixed rail and rapid bus transit routes, as well as on-demand shuttles. While the trains and buses operate on a fixed schedule, the shuttles are routed dynamically in real time. The example path through the ODMTS involves a shuttle leg to pick up the rider, a rail leg, a bus leg, and a final shuttle leg to bring the rider to her destination. All these legs are synchronized: for instance, the shuttle serving the last leg is waiting at the bus stop to bring the rider to her final destination. This video describes this process in more detail (Socially Aware Mobility Lab, 2020).

Real-world case studies of ODMTS systems have repeatedly found that ODMTS have the potential to cut costs and improve passenger convenience. Mahéo et al. (2019) present a case study for Canberra, Australia, for which the current network comprises about 2800 bus stops, and which sees about 60,000 passengers per day. ODMTS simulations have been performed for the transit system of the University of Michigan, and some of the results have been validated by a pilot in the Spring of 2018 (Van Hentenryck, 2019). Basciftci and Van Hentenryck (2020, 2021) and Auad and Van Hentenryck (2021) study the Ann-Arbor/Ypsilanti region in Michigan, which currently consists of 1267 bus stops, and the case studies consider about 3000 up to 7000 passengers at a time. Dalmeijer and Van Hentenryck (2020) present results for 7167 riders of the MARTA system in Atlanta, which currently consists of 5563 bus stops and 38 rail stations. Aside from cutting cost and improving passenger convenience, other advantages of ODMTS and its contribution to social mobility are discussed by Van Hentenryck (2019).

To study the resiliency of ODMTS to the effects of depressed ridership and additional safety requirements that arise during a pandemic, an ODMTS is designed for the city of Atlanta, and its performance is evaluated under different scenarios that capture various stages of the pandemic. The evaluation is based on a detailed simulation that uses real transit data provided by MARTA. The contributions of the paper can be summarized as follows:

- 1. The paper presents a pipeline for designing and evaluating an ODMTS, combining advanced models for trip chaining, ODMTS design, ridesharing and fleet sizing, and real-time shuttle dispatching for the first time. These models are adapted to operate in a multimodal setting, and to satisfy practical constraints. In particular, the models impose a constraint on the number of passenger transfers, and a new network design model is introduced to avoid the computational burden imposed by this constraint.
- 2. The paper provides a comprehensive case study for the city of Atlanta to assess the resiliency of ODMTS under various scenarios of pandemic response, which include loss of revenue due to depressed demand and reduced vehicle capacity due to social distancing requirements. High-fidelity simulations show that, by scaling down the number of shuttles appropriately, an ODMTS provides a similar level of service with a cost savings that compensates for revenue losses. The case study also shows that an ODMTS can operate successfully under more restrictive budgets, at the cost of increasing waiting times during the busiest times of the day.



Fig. 2. The MARTA rail network (MARTA, 2020).

This rest of the paper is structured as follows. Section 2 presents related work in the literature, and Section 3 reviews the current MARTA transit system and its response to the pandemic. The pipeline for designing and evaluating an ODMTS is presented in Section 4. Section 5 introduces an ODMTS for Atlanta, and its resiliency is tested in Section 6. The final section summarizes the findings and presents directions for future research.

2. Related work

Recent work has focused on understanding the impact of COVID-19 on public transit ridership. Liu et al. (2020) provide a systematic analysis of 113 public transit systems across the U.S., using data from the Transit App to study the unprecedented decline of public transit during this pandemic. They explored how social distancing, self-quarantine, and working from home recommendations from the Center for Disease Control and Prevention (CDC) impacted ridership, even before the local spread of COVID-19. Tirachini and Cats (2020) discuss factors that influence the contagion risk of COVID-19 in public transit, including vehicle and station occupancy, exposure time, mask use, and hygiene. COVID-19 has led to new challenges for the transportation community, and different examples are given in the survey by Agatz et al. (2021). Gkiotsalitis and Cats (2021b) study the impact of COVID-19 on public transit, and survey methods for public transit planning that can be used to address the changes in demand patterns and reductions in capacity. These include methods to set service frequencies, modify timetables, and to prevent crowding. Changing the service frequencies depending on the social distancing requirements has been studied by Gkiotsalitis and Cats (2021a). The authors develop a mixed-integer quadratic programming model, which is used to conduct a case study for the Washington D.C. metro network.

The interaction between multimodal networks and on-demand vehicles has been considered by Salazar et al. (2018), who look into the coordination of public transit systems with fleets of autonomous vehicles and its benefits. Their case study is based on New York City and the existing public transit system. Pinto et al. (2020) focus on the allocation of resources between public transit fleets and shared-use autonomous mobility services. They choose the frequency of the public transit routes and size of the fleet in a bilevel problem under a constrained budget. A case study is provided for the city of Chicago.

3. The MARTA transit system

The MARTA transit system consists of trains and buses that cover Fulton, Clayton, and DeKalb counties in the metro Atlanta area. The rail network consists of 38 stations and four lines: the Green, Blue, Red, and Gold line (Fig. 2). With around 160,000 transactions on a typical weekday, this is the 8th largest rail network in the US by ridership. In addition to the rail, MARTA operates over 500 buses that serve over 110 different lines, and see approximately 110,000 transactions every day. Fig. 3 shows the total bus and rail coverage, the rail being the backbone of the system. The network is overlayed on a map of population densities (Atlanta Regional Commission, 2019).

According to the U.S. Census Bureau (2020), the rate of public transit commuting to work in Atlanta is 10.4%; in contrast, NYC and Boston have rates of 56.0% and 33.3%, respectively. Atlanta is also routinely ranked among the most congested cities in the

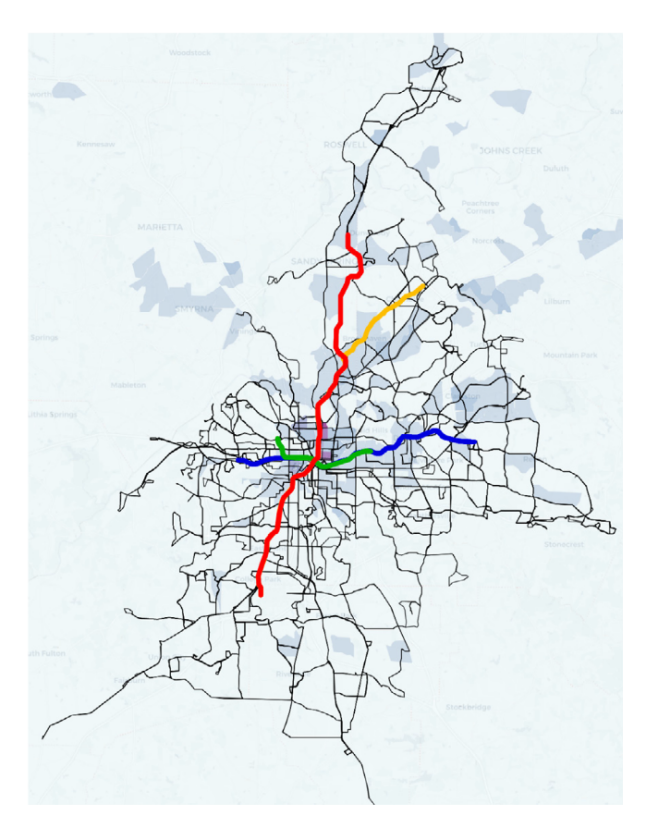


Fig. 3. The MARTA bus and rail coverage in 2019.

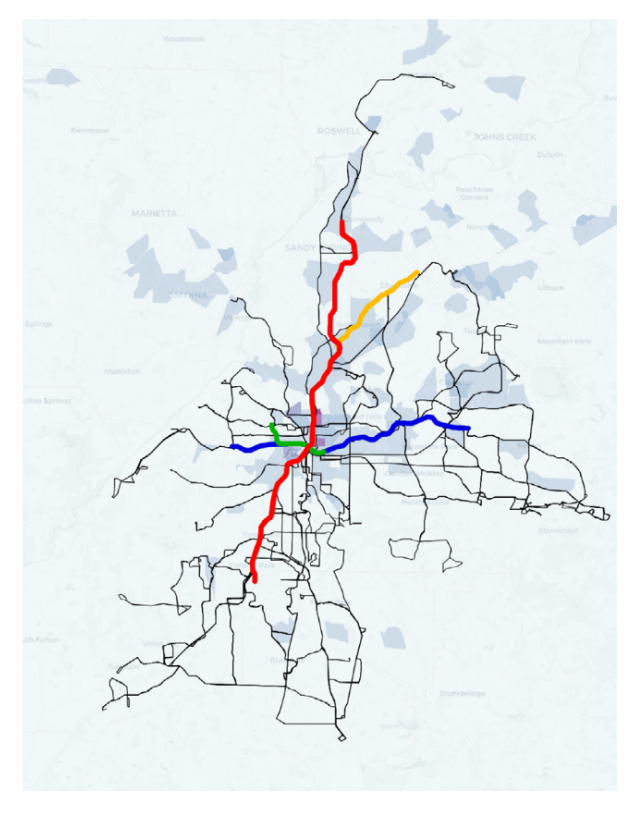


Fig. 4. The MARTA essential service plan.



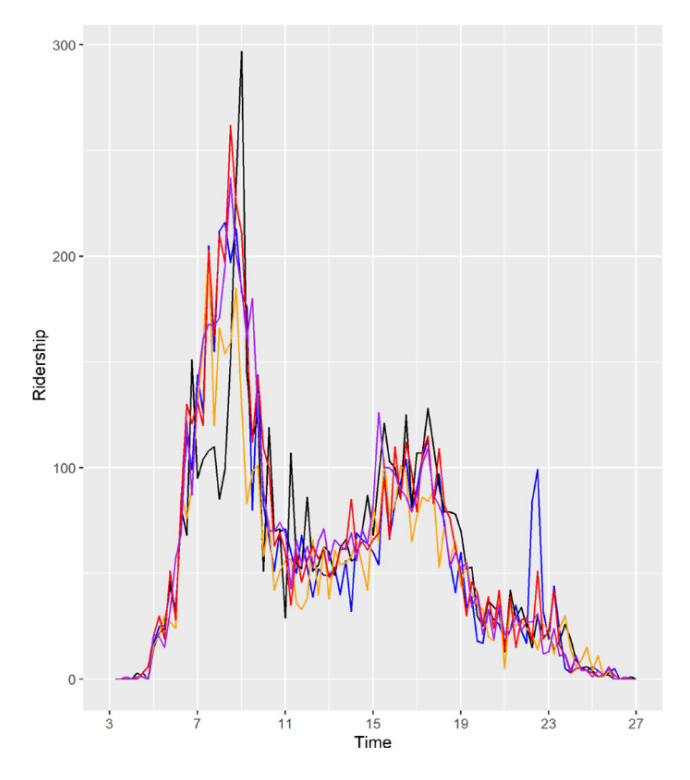


Fig. 5. Arrivals at North Avenue station per 15 min interval (first five weekdays of March 2019).

world. The INRIX Traffic Scorecard ranks Atlanta to be the 10th most congested city in the US, with 82 lost hours per year for the average driver (Reed, 2019). Still, it is reported that driving typically results in a shorter commute than using public transit. This is in line with Fig. 3, which shows that the public transit network spans a large geographical area, but is also sparse in many regions, which prevents convenient access.

3.1. Ridership data

To access the MARTA system, riders use a transit pass, known as the *Breeze Card*. Passengers tap their Breeze Card when boarding a bus and when entering and exiting a rail station. Inside buses, riders can also pay with cash. The Breeze Card *transaction data* is collected by the Automated Fare Collection (AFC) system, which records the time and type of the transaction, the terminal at which the transaction took place, and the Breeze Card id (if applicable). In addition to transaction data, MARTA collects *Automated Passenger Counter (APC) data* in the MARTA buses, using cameras or infrared beams in the doorways to record boardings and alightings. For every stop, the data contains the number of boardings and alightings, the vehicle id, the route and direction, and the time and duration of the stop. This data is supplemented with GPS coordinates from the Automatic Vehicle Location system.

For the case study, transaction data and APC data for 2018 are combined to create a set of 192,311 passenger trips that is representative for an average weekday in March 2018. Details on estimating the origin-destination matrix are provided in Section 4.1. The case study focuses on the 55,871 passengers traveling during the 6am-10am morning peak, which is one of the most challenging periods of the day. Transaction data collected during the pandemic has been made available for March up to May 2020. To study the effect of the pandemic on ridership, the same data was provided for the year before. Ridership over the day is typically very predictable. As an example, Fig. 5 presents the number of passengers arriving at North Avenue station per 15 min interval for consecutive weekdays in March 2019, which shows that demand under normal circumstances is quite stable, even for short time intervals and at the station level.

3.2. Cost and performance

The Federal Transit Administration (2018) provides details on MARTA's financials. In 2018, operating and capital expenses were \$591M and \$244M, respectively. Most operating costs stem from the bus network (49%) and the rail (44%); the remainder is for paratransit services for passengers. Fares and directly generated funds, which are most affected during a pandemic, pay for 33% of the operating budget.

MARTA reports an average operating expense of \$104.10 per bus revenue hour, which includes costs for general administration and facility maintenance, but excludes depreciation of the vehicles. For the case study, it is important to know how the cost of operating a bus compares to the cost of operating a shuttle. To present a fair comparison, this paper focuses only on the main cost

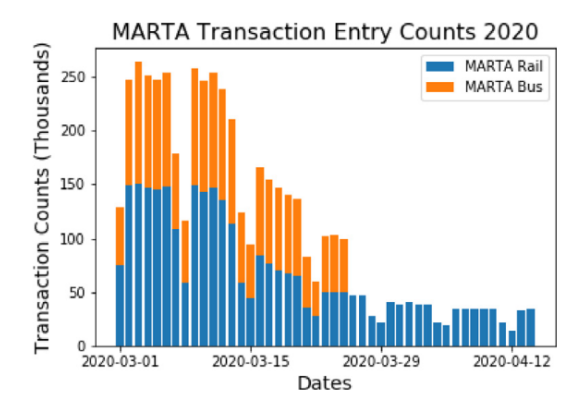


Fig. 6. Breeze Card tap-ins from March to mid-April 2020 (Bus transactions were not recorded after March 26).

differentiators: labor cost, vehicle maintenance cost, and depreciation cost. This puts the hourly cost of a bus at \$72.15. MARTA operates 465 buses in maximum service, which results in a daily cost of \$134k during the four hour morning peak. Details on this cost calculation are provided by the Appendix.

In terms of performance, the data shows that waiting times are relatively long, especially for bus users. The average duration for morning-peak trips that include a bus is 46 min: 20 min of travel time and 26 min of waiting time. The travel time is calculated from the transaction data, and the waiting time is estimated based on the service frequencies. Even without traffic, the average trip duration would still be 40 min for these passengers. The situation is better for riders only using rail: their trips take 25 min on average. Note that the time to get to the bus stop or rail station is not included in this calculation, which means that the actual trips take longer.

3.3. Pandemic response

In March 2020, COVID-19 cases were increasing rapidly. MARTA responded by implementing a series of hygiene protocols and by reducing the maximum occupancy of buses and trains, following new guidelines by the CDC. The following is a brief timeline of events during March and April 2020:

- March 11th: the World Health Organization characterized the novel coronavirus outbreak as a pandemic (World Health Organization, 2020);
- March 26th: MARTA required passengers to enter buses through the rear door, and fare collection was suspended to accommodate this;
- March 30th: MARTA reduced the frequency of its bus schedule;
- April 20th: MARTA switched to an essential service plan consisting of 41 bus routes.

Additionally, the rail frequencies were reduced during this period (Atlanta Regional Commission, 2020).

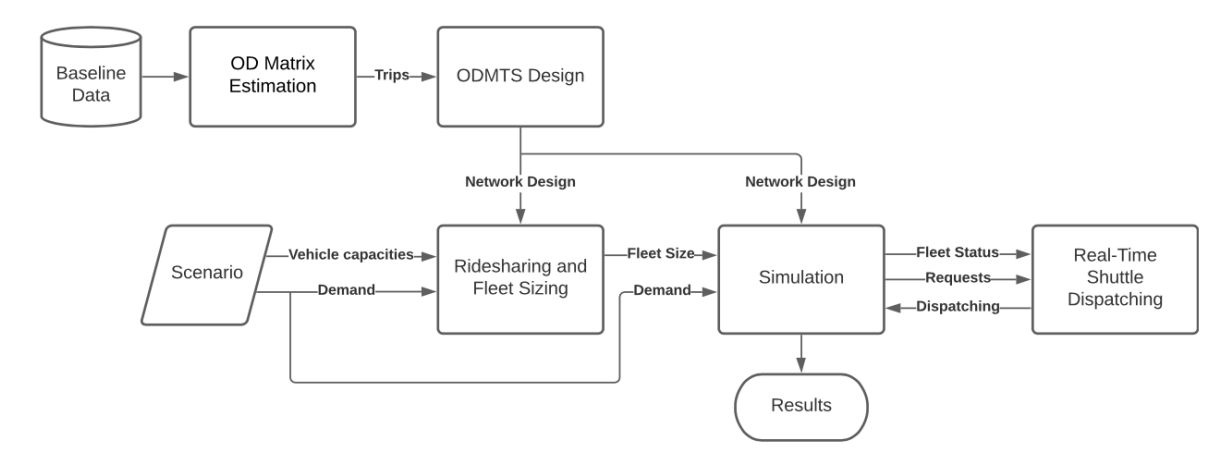
Following the spread of COVID-19, public transit ridership collapsed due to lockdowns and social distancing, and many people have started working from home. Fig. 6 shows how the number of bus and rail transactions decreased during March and April 2020. The ridership at the beginning of March was similar to that of 2019, and represented a typical demand. Late March, bus ridership had decreased by roughly 50%, and rail ridership was reduced by approximately 70%. On March 26, bus fare collection was suspended, and no more transactions were recorded. In April, rail ridership was at around 22% of the normal level, and bus ridership was down by 51% on April 19 (see MARTA performance indicators). Ridership remained low thereafter, with similar numbers for May.

MARTA's essential service plan was introduced to provide safer service on its most critical routes, while dealing with rapidly declining ridership, additional cleaning requirements, and new social distancing policies. It cut many routes that were assessed as "less-critical". Fig. 4 shows the bus and rail coverage of the essential service plan, and compared to Fig. 3, it is clear that public transit is less accessible during the pandemic. Although this was necessary, switching to the essential service plan did have a significant negative impact on many people of Atlanta (Wickert, 2020a).

4. ODMTS

This section reviews the software pipeline for designing an ODMTS and evaluating its cost and performance. The pipeline provides an end-to-end solution by bringing together recent methods for demand estimation, network design, fleet sizing, real-time dispatching, and simulation, and adapting them to work in a multimodal setting. Fig. 7 presents an overview of the pipeline, and Table 1 summarizes the nomenclature used in this section.

The network design of an ODMTS takes as input an Origin-Destination (O-D) matrix which is estimated from the baseline data and represents rider trips, as well as a set of hubs that can be connected by rail or buses. The design indicates which connections are served by buses, rail, or shuttles, as well as the frequencies for the fixed lines. The ridesharing and fleet-sizing optimizations



 $\textbf{Fig. 7.} \ \ \textbf{Pipeline for the design and evaluation of ODMTS}.$

Table 1

Nomenclature.	
Symbol	Definition
Sets	
V	Set of locations
V_H	Set of transit hub locations, $V_H \subseteq V$
M	Set of modes, $M = \{shuttle, bus, rail\}$
F^m	Set of frequencies for mode $m \in \{bus, rail\}$ (possible number of vehicles over the time horizon)
\boldsymbol{A}	Set of arcs, each $a \in A$ represents traveling from $i(a) \in V$ to $j(a) \in V$ with mode $m \in M$ and frequency $f(a) \in F^m$
A^{bus}	Set of bus arcs, $A^{bus} \subseteq A$
P	Set of shuttle requests, each $p \in P$ consists of an origin, destination, and request time
T	Set of trips, each $t \in T$ consists of an origin $o(t) \in V$, destination $d(t) \in V$, number of passengers $p(t)$
P_h^+ $P_h^ P_{direct}$	Shuttle requests with hub $h \in V_H$ as the origin, $P_h^+ \subseteq P$
P_b^{-}	Shuttle requests with hub $h \in V_H$ as the destination, $P_h^- \subseteq P$
P_{direct}^{n}	Shuttle requests that do not involve a hub, i.e., $P_{direct} = P \setminus P_H$
R_h^+	Set of shuttle routes that only serve requests in P_h^+
$R_h^{\frac{n}{-}}$	Set of shuttle routes that only serve requests in P_h^-
$s^{''}$	Set of shuttles, each $s \in S$ is associated with a current time and location
R_s	Set of shuttle routes that can be performed by shuttle $s \in S$
R	Shuttle routes considered by the dispatching algorithm, $R = \bigcup_{s \in S} R_s$
Parameters	Jacob Color
α	Weight parameter that assigns weight α to total trip duration and $(1-\alpha)$ to system cost, $\alpha \in [0,1]$
τ_a	Time to travel arc $a \in A$
d_a	Distance to travel arc $a \in A$
c ^m	Hourly cost of operating one vehicle of mode $m \in M$
$\bar{c}^{shuttle}$	Estimated shuttle cost per mile used by the network design algorithm
L	Length of the time horizon
L ⁺	Length of the extended time horizon used to get accurate results over the time horizon
β_a	Cost of including arc $a \in A^{bus}$ in the design, $\beta_a = (1 - \alpha)\tau_a f(a)e^{bus}$
	Cost of traversing arc $a \in A$ for trip $t \in T$, $\gamma_a^t = p(t) \left((1 - \alpha) d_a \bar{c}^{shuttle} + \alpha \tau_a \right)$ for shuttle, $\gamma_a^t = p(t) \alpha \left(\tau_a + \frac{L}{2f(a)} \right)$ for bus and rail
γ_a^i	\
K	Maximum number of arcs traveled by each passenger, $K \ge 1$, corresponds to $K - 1$ transfers
γ^r	Cost of shuttle route $r \in R_H$ as used by the ridesharing algorithm
ρ	Tolerance factor for shuttle trips in the ridesharing algorithm
Δ	Time window width to allow for ridesharing in the ridesharing algorithm
b_p^r	Indicator that is one if shuttle route r covers shuttle request $p \in P$, and zero otherwise
Q^m	Maximum number of passengers in one vehicle of mode $m \in M$
1	Length of a dispatching epoch
c_r	Cost of shuttle route $r \in R$ as used by the dispatcher, equal to sum of the waiting times
g_p	Penalty for not serving request $p \in P$ in the current epoch
\bar{g}	Initial penalty for not serving request $p \in P$, based on zero waiting time
Variables	
z_a	One if arc $a \in A^{bus}$ is part of the network design, zero otherwise
y_a^t	One if trip $t \in T$ uses arc $a \in A$ in the network design, zero otherwise
x_r	One if shuttle route r is selected in the ridesharing solution, zero otherwise
$f_{(r,r')}$	One if shuttle routes $r, r' \in R_H$ are served sequentially by the same shuttle in the fleet-sizing algorithm, zero otherwise
θ_r	One if shuttle route $r \in R$ is selected by the dispatcher, zero otherwise
w_p	One if shuttle request $p \in P$ is unserved in the current solution by the dispatcher, zero otherwise

	7	

then determine the necessary number of shuttles. Based on the network design, the fleet size, and the demand, a *real-time simulation* mimics real-time operations. It keeps track of every rider and every vehicle over time, including their positions over time, the trip legs for riders, the vehicle occupancies, and the unserved requests. The real-time dispatching and routing of the shuttles is performed using an optimization algorithm over a rolling horizon: the optimization is run every 30 s on requests that have been batched in the previous time periods or have not been served yet. This leads to a high-fidelity evaluation of the ODMTS.

The simulator obviously depends on its inputs, but is independent from the models and assumptions that are used to generate these inputs. In Section 4.2, for example, vehicle capacity are ignored while creating the design, but the simulator enforces that passengers wait for the first vehicle with an empty seat. Modeling choices are thus made during network design and fleet sizing, but they do not impact how the system is evaluated. Capacity could be incorporated in the network design, but this is not needed in practice, since the large vehicles are almost never used at capacity.

To evaluate the resilience of an ODMTS, this paper makes use of *scenarios*. Each scenario defines the vehicle capacities (e.g., to enforce social distancing policies), the frequencies, and the demand for public transit. Varying these inputs allows for evaluating both pandemic and non-pandemic scenarios. The scenarios focus on large shifts in demand due to the pandemic, rather than the daily variations which are very small in comparison. The base scenario is the proposed ODMTS network designed for the estimated O–D matrix for the current system. Improving the quality of service may attract new demand, which counteracts some of the decrease. This effect is studied by Basciftci and Van Hentenryck (2021). A similar analysis could be performed for the case study in this paper. However, this would require the development of new choice models to capture mode switching during a pandemic, which is a significant undertaking and is left for future research.

4.1. O-D matrix estimation

This paper uses techniques by Barry et al. (2002) to estimate the O-D matrix from the transaction data and the APC data. Transactions are first grouped into *legs*, a leg being a part of a trip where the rider is in a single bus or in the rail system. After establishing the individual legs, the legs are chained into trips, and trip destinations are estimated when data is unavailable. This occurs because the transactions (obtained from the Breeze Cards) report tap-in and tap-out data for the trains, but only tap-in data for the buses. However, since the ridership mostly consists of commuters, it is generally possible to infer the bus destination for a morning trip by using the corresponding bus boarding of the evening trip (and vice versa). The remaining destinations can be estimated by using the APC data and ensuring that the distributions match under some reasonable assumptions. The result is a set of rider trips T, where each trip $t \in T$ is represented by an origin o(t), a destination d(t), and the number of riders p(t).

4.2. ODMTS design

The network design uses a new optimization model that refines the model introduced by Mahéo et al. (2019) to capture transfer constraints, multiple frequencies, and additional transportation modes.¹ The design problem chooses the fixed routes and their frequencies, minimizing a weighted combination of fixed and operation costs, and trip durations. Its solution implicitly defines the legs taken by every rider.

Problem description The design problem is defined in terms of a directed multigraph G = (V, A) and a set of trips T. Vertices in V represent geographical locations, and arcs in A are possible connections for the ODMTS design. Arc $a \in A$ captures the possibility of traveling from origin $i(a) \in V$ to destination $j(a) \in V$ with mode $m(a) \in M$, where $M = \{shuttle, bus, rail\}$. Bus and rail arcs have a frequency $f(a) \in F^{bus}$ and $f(a) \in F^{rail}$ respectively. Bus and rail arcs provide the connections between a set of transit hubs $V_H \subseteq V$, while shuttles provide the connections to and from the hubs. Designing the network amounts to choosing which arcs $a \in A$ to open. The shuttle arcs $a \in A$ capture that passengers are transported from i(a) to j(a) by shuttles, but the network design model does not specify how the shuttles perform this task. Shuttle routes will be created dynamically as part of the simulation by the real-time shuttle dispatcher (Section 4.4) to ensure a realistic evaluation of the system.

This paper assumes that the rail network is fixed and that shuttle connections can always be used, such that rail and shuttle arcs are always opened. More precisely, the arc set A is constructed as follows. Note that G is a multigraph, and allows for parallel arcs corresponding to different modes and frequencies. Rail arcs are added with a fixed frequency between every pair of stations that is connected by a rail line, and it is assumed that all rail stations are in V_H . Shuttle connections are added for every trip: from the origin to the hubs, from the hubs to the destination, and directly from the origin to the destination. Bus arcs are added for all frequencies in F^{bus} between all bus-only hubs (hubs that are not rail stations) and between each bus-only hub and the three nearest rail stations. The set of all bus arcs is denoted by A^{bus} . What remains to decide is which bus connections to provide and at which frequencies.

The objective of the design problem is to minimize a weighted combination of *fixed and variable costs* and *trip duration*, with parameter $\alpha \in [0,1]$ used to balance these objectives. The cost is given the weight $1-\alpha$ and the total trip duration, i.e., the total travel and waiting times, is given the weight α . The fixed cost for including a bus arc $a \in A$ is defined as $\beta_a = (1-\alpha)\tau_a f_a c^{bus}$, i.e., the product of travel time τ_a , the number of buses over the time horizon f_a , and hourly bus cost c^{bus} .

¹ A preliminary model was presented at the CPAIOR 2020 conference (Dalmeijer and Van Hentenryck, 2020).

The contribution to the objective of trip $t \in T$ traveling over arc $a \in A$ is given by

$$\gamma_a^t = \begin{cases} p(t) \left((1 - \alpha) d_a \bar{c}^{shuttle} + \alpha \tau_a \right) & \text{if } m(a) = shuttle \\ p(t) \alpha \left(\tau_a + \frac{L}{2f(a)} \right) & \text{if } m(a) \in \{bus, rail\}. \end{cases}$$
 (1)

The product $d_a \bar{c}^{s huttle}$ represents the variable cost of using a shuttle along a, obtained by multiplying the distance by the shuttle cost per mile. This cost of using shuttle arc a is an approximation for the actual cost of transporting a passenger from i(a) to j(a) when operating a real-time ride-sharing system (Section 4.4).

The contribution to the trip duration is τ_a , since the shuttles are assumed to be available within a short waiting time. There are no variable costs associated with using a bus or a train. The contribution to the trip duration is the sum of the travel time and the expected waiting time. This value is calculated from the length of the time horizon L and the number of departures during that time.

Because transfers discourage people from using the ODMTS, a limit of $K \ge 1$ legs is imposed on the length of each passenger path. This ensures that the total number of transfers is at most K-1, which occurs when the passenger has to change vehicles between every pair of arcs. Vehicle capacity is not considered at the network design stage, motivated by the currently low utilization in Atlanta, but is still taken into account by the simulator. Section 5 shows that, for the case study, there is indeed no need to consider capacities, as passengers in the simulation almost always find an empty seat.

Optimization model The decision variables of the model are specified as follows: Variable $z_a \in \mathbb{B}$ is a binary variable with value one if and only if bus arc $a \in A^{bus}$ is part of the design, while flow variable $y_a^t \in \mathbb{B}$ indicates that the passengers of trip $t \in T$ travel through arc $a \in A$. Formulation (2) presents the model. For brevity, $\delta^+(i)$ denotes the set of outgoing arcs for $i \in V$, and $\delta^+(i, m)$ the set of outgoing arcs for $i \in V$ restricted to mode $m \in M$. The sets $\delta^-(i)$ and $\delta^-(i, m)$ are defined similarly for incoming arcs.

$$\min \qquad \sum_{a \in A^{bus}} \beta_a z_a + \sum_{t \in T} \sum_{a \in A} \gamma_a^t y_a^t, \tag{2a}$$

$$\text{s.t.} \quad \sum_{a \in \delta^+(i,bus)} f(a)z_a - \sum_{a \in \delta^-(i,bus)} f(a)z_a = 0 \qquad \qquad \forall i \in V_H, \tag{2b}$$

$$\sum_{a \in A^{bus} \mid i(a)=i} z_a \le 1 \qquad \forall i, j \in V_H, \tag{2c}$$

$$\begin{aligned} z_{a} - \sum_{a \in \delta^{-(i,bus)}} f(a) z_{a} &= 0 & \forall i \in V_{H}, \\ \sum_{a \in A^{bus} \mid i(a) = i, j(a) = j} z_{a} &\leq 1 & \forall i, j \in V_{H}, \\ \sum_{a \in \delta^{+}(i)} y_{a}^{t} - \sum_{a \in \delta^{-}(i)} y_{a}^{t} &= \begin{cases} 1 & \text{if } i = o(t) \\ -1 & \text{if } i = d(t) \end{cases} & \forall t \in T, i \in V, \end{aligned}$$

$$(2c)$$

$$y_{a}^{t} \le z_{a} \qquad \forall t \in T, a \in A^{bus},$$
 (2e)

$$y_{a}^{t} \leq z_{a} \qquad \forall t \in T, a \in A^{bus},$$

$$\sum_{a \in A} y_{a}^{t} \leq K \qquad \forall t \in T,$$

$$y_{a}^{t} \in \mathbb{B} \qquad \forall t \in T, a \in A,$$

$$(2e)$$

$$(2f)$$

$$y_a^t \in \mathbb{B} \qquad \forall t \in T, a \in A,$$
 (2g)

$$z_a \in \mathbb{B} \qquad \forall a \in A^{bus}. \tag{2h}$$

Objective (2a) minimizes the cost for selecting bus arcs, and the total passenger objective. Constraints (2b) balance the number of incoming and outgoing buses at every hub, while Constraints (2c) ensure that at most one bus frequency is selected for every connection. Standard flow conservation constraints for the passenger trips are given by Constraints (2d). Passengers only use bus arcs that are part of the design, as stated by Constraints (2e). The transfer limit constraint is enforced by Constraints (2f), and Eqs. (2g)-(2h) are the integrality requirements.

Benders decomposition Mahéo et al. (2019) apply Benders decomposition to exploit the structure of the ODMTS design problem, and the same decomposition is used in this paper. The master problem determines the design by selecting bus arcs, and the subproblem routes the riders through the network. Let $\Phi(z)$ be the optimal value for the variable cost of the objective value given the values of the design variables z. The master problem is given by Formulation (3), and Formulation (4) presents the subproblem. The master problem concerns the design variables, and the passenger cost resulting from the design is implicitly defined through $\Phi(z)$. The continuous variable θ is introduced for notational convenience, and equals $\Phi(z)$ in any optimal solution. For a given design z, the subproblem is separable, and the problem of routing the riders through the network can be solved for each trip independently, which is a significant computational advantage.

$$\min \sum_{a \in A^{bus}} \beta_a z_a + \theta, \tag{3a}$$

s.t. (2b), (2c), (2h),

$$\theta \ge \Phi(z),$$
 (3b)

$$\theta \ge 0.$$
 (3c)

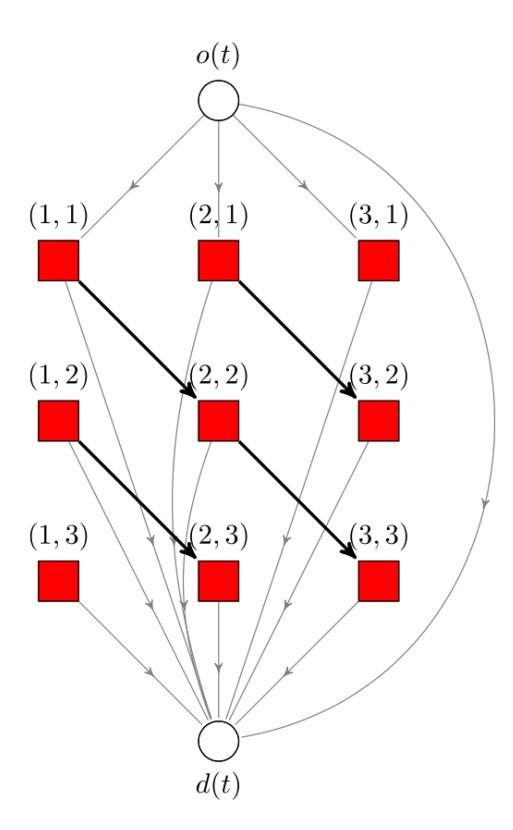


Fig. 8. Example of a transfer-expanded graph for K = 4 and two hub arcs in the original graph.

$$\Phi(z) = \min \sum_{t \in T} \sum_{a \in A} \gamma_a^t y_a^t,$$
s.t. (2d)-(2g). (4a)

Benders approaches construct an outer-approximation of Constraint (3b), which is the epigraph of $\Phi(z)$, by iteratively solving the master problem for the current approximation, and then solving the subproblem to obtain a supporting hyperplane at the current value of z. Mahéo et al. (2019) show for their model that the subproblem is totally unimodular, which justifies the approach.

The new model (2), however, is complicated by the transfer limit constraint (2f), which destroys total unimodularity and results in $\Phi(z)$ being non-convex. Handling non-convex value functions has been addressed in the literature (Laporte et al., 2002; Codato and Fischetti, 2006), but significantly increases the computational complexity. To remedy this limitation, the next section introduces an alternative formulation for the subproblem that enforces the transfer limit without destroying total unimodularity, so that a standard Benders decomposition method can be applied.

Transfer-expanded graphs To maintain total unimodularity in the subproblem, this section reformulates the subproblem on a transfer-expanded graph. Transfer-expanded graphs are layered graphs for which each layer corresponds to a number of transfers. The transfer limit constraint is encoded directly by limiting the number of layers in the graph. Transfer-expanded graphs share some similarities with time-expanded networks, where layers are used to represent different periods of time. A literature review on time-expanded graphs is given by Boland et al. (2017), and a more general discussion on layered graph approaches is presented by Gouveia et al. (2019).

For clarity, the transfer-expanded graph is introduced for a given trip $t \in T$ (recall that the subproblem is separable). Let $\bar{G} = (\bar{V}, \bar{A})$ denote the transfer-expanded graph. The vertex set \bar{V} consists of the origin o(t), the destination d(t), and K-1 copies of each hub, denoted by (i,k) for $i \in V_H$ and $k \in \{1, ..., K-1\}$. The arc set \bar{A} is constructed as follows. Fig. 8 provides an illustrative example.

- For every arc $a \in A$ between the hubs, add K-2 copies to \bar{A} , each going from one layer to the next. That is, add $\bar{a} = ((i(a),k),(j(a),k+1))$ for every $k \in \{1,\ldots,K-2\}$.
- Add $\bar{a} = (o(t), d(t))$ for the direct shuttle connection.
- Add shuttle arcs from the origin to the first layer of hubs, $\bar{a} = (o(t), (i, 1))$ for $i \in V_H$.
- Add shuttle arcs from every layer of hubs to the destination, $\bar{a} = ((i, k), d(t))$ for $i \in V_H$, $k \in \{1, \dots, K-1\}$.

By construction, there is a bijection between paths in the transfer-expanded graph and paths in the original graph that satisfy the transfer limit constraint. This allows the subproblem to be formulated as a standard shortest path problem on the transfer-expanded

graph. With a slight abuse of notation, let the cost γ_a^i of arc $\bar{a} \in \bar{A}$ be equal to γ_a^i for the associated arc $a \in A$ in the original graph. The binary variables y_a^i indicate the passenger flow through the transfer-expanded graph. For notational convenience, let $\bar{A}(a)$ denote the copies of arc $a \in A$ in the transfer-expanded graph, and let $\bar{\delta}^+(\bar{v})$ and $\bar{\delta}^-(\bar{v})$ denote the outgoing and incoming arcs, respectively, for $\bar{v} \in \bar{V}$. Model (5) presents the new formulation for the subproblem. Objective (5a) calculates the passenger cost in the same way as the original subproblem, and Constraints (5b) are the equivalent of the flow conservation constraints (2d). Constraints (5c) ensure that copies of bus arcs in the transfer-expanded graph can only be used if the original arc is part of the design. Finally, Eqs. (5d) define the passenger flow variables. It is important to observe that the original transfer limit constraint (2f) is encoded directly in the structure of the graph, and no additional constraint is needed. The resulting subproblem is a minimum-cost flow problem, which has a totally unimodular constraint matrix, such that the integrality conditions (5d) may be relaxed.

$$\min \qquad \sum_{t=1}^{\infty} \gamma_{t}^{t} y_{d}^{t}, \tag{5a}$$

a totally unimodular constraint matrix, such that the integrality conditions (5d) may be relaxed.

min
$$\sum_{\bar{a}\in\bar{A}}\gamma_{\bar{a}}^t y_{\bar{a}}^t, \qquad (5a)$$
s.t.
$$\sum_{\bar{a}\in\bar{\delta}^+(\bar{v})} y_{\bar{a}}^t - \sum_{\bar{a}\in\bar{\delta}^-(\bar{v})} y_{\bar{a}}^t = \begin{cases} 1 & \text{if } \bar{v}=o(t) \\ -1 & \text{if } \bar{v}=d(t) \end{cases} \quad \forall \bar{v}\in V, \qquad (5b)$$

$$y_{\bar{a}}^t \leq z_a \qquad \forall a\in A^{bus}, \bar{a}\in\bar{A}(a), \qquad (5c)$$

$$y_{\bar{a}}^t \in \mathbb{B} \qquad \forall \bar{a}\in\bar{A}. \qquad (5d)$$

$$y_{\bar{a}}^t \le z_a \qquad \forall a \in A^{bus}, \bar{a} \in \bar{A}(a),$$
 (5c)

$$y_{\bar{a}}' \in \mathbb{B} \qquad \forall \bar{a} \in \bar{A}.$$
 (5d)

The Benders decomposition method is applied as follows. Let $\bar{\Phi}(z)$ be the optimal objective value of the subproblem defined on transfer-expanded graphs, which replaces $\Phi(z)$ in the master problem. The constraint $\theta \ge \bar{\Phi}(z)$ is enforced by adding cutting planes. For every $\hat{z} \in [0,1]^{|A^{bus}|}$, the standard *Benders cut* (Benders, 1962) is given by

$$\theta \ge \bar{\boldsymbol{\Phi}}(\hat{z}) + \sum_{t \in T} \sum_{a \in A} \left(\sum_{\bar{a} \in \bar{A}(a)} \mu_{\bar{a}}^{t}(\hat{z}) \right) (z_{a} - \hat{z}_{a}), \tag{6}$$

where $\mu_{\bar{c}}^{l}(\hat{z})$ are optimal dual values for Constraints (5c), obtained by solving the subproblem for trip t for design \hat{z} . The network design problem is solved by repeatedly solving the current master problem, solving the independent subproblems to generate a Benders cut, and adding the cut to the master problem. When no more cuts are violated, the problem is solved to optimality. In this paper, the master problem is solved with CPLEX, and Benders cuts are separated in callbacks for both fractional and integer solutions \hat{z} . The subproblems are solved with the LEMON graph library (Dezső et al., 2011).

4.3 Ridesharing and fleet sizing

Once the network is designed, the next step in the optimization pipeline is to derive the appropriate size for the shuttle fleet. This paper follows the same approach to fleet sizing as Auad and Van Hentenryck (2021), who study the impact of ridesharing and fleetsizing on ODMTS more generally. The fleet sizing proceeds in two steps: it first identifies ridesharing opportunities using a ridesharing optimization, before applying the fleet-sizing optimization. The ridesharing optimization constructs minimum-cost shuttle routes that cover the passenger shuttle requests, and the fleet-sizing optimization finds the minimum number of shuttles to cover these routes. Both algorithms use the extended time horizon L^+ to prevent that the fleet size is underestimated near the end of the time horizon.

The ridesharing optimization Let P be a set of shuttle requests, where each request $p \in P$ belongs to a single passenger and consists of an origin, a destination, and a request time. The set P is obtained from the shortest paths through the designed network of all trips. It contains a request for every shuttle arc used by riders. If the request is at the start of the trip, then the starting time of the trip is used as the request time. If this is not the case, the request time is obtained by following the path. The shuttle requests are partitioned based on the request type: for every hub $h \in V_H$, P_h^- is the set of requests with destination h and P_h^+ the set of requests with origin hub h. The remaining requests, that correspond to direct shuttle trips, are denoted by P_{direct} .

The objective of the ridesharing optimization is to construct shuttle routes that cover all requests and minimize the total cost. Riders are eligible to share the same shuttle if (i) the number of passengers does not exceed the vehicle capacity Qshuttle; (ii) their departure times fall within a time window of width $\Delta \geq 0$; (iii) all the passenger either travel towards the same hub or depart from the same hub (i.e., requests are in the same set P_h^- or P_h^+); and (iv) the duration of their shared route does not exceed the duration of a direct trip by a factor more than tolerance $\rho \ge 1$.

The route enumeration algorithm by Auad and Van Hentenryck (2021) is used to construct the sets R_h^- and R_h^+ of feasible routes for every hub $h \in V_H$. Routes in sets R_h^- and R_h^+ are based on requests from P_h^- and P_h^+ respectively. A route starts when an empty shuttle picks up passengers, and ends when the last passenger is dropped off. Every shuttle route is associated with a starting time and an ending time. The starting time is the latest request time among the passengers on the route, which ensures that the route can only be started when all passengers are ready. The ending time follows from adding the route duration to the starting time. The cost of shuttle route r is given by the parameter γ^r , which is the same weighted sum of shuttle cost and passenger trip duration used for designing the ODMTS.

The ridesharing optimization is solved as independent set partitioning problems for every route set R_h^- and R_h^+ associated with every hub. Without loss of generality, the formulation is presented for the route set R_h^- and the corresponding requests P_h^- . Let

 $x_r \in \mathbb{B}$ be a binary variable that takes the value of one if route $r \in R_h^-$ is selected, and zero otherwise. The binary parameter b_p^r is set to one if route $r \in R_h^-$ contains request $p \in P_h^-$, and zero otherwise.

$$\min \sum_{r \in R_h^-} \gamma^r x_r, \tag{7a}$$

$$\min \sum_{r \in R_h^-} \gamma^r x_r,$$

$$\text{s.t.} \quad \sum_{r \in R_h^-} b_p^r x_r = 1 \quad \forall p \in P_h^-,$$

$$(7a)$$

$$x_r \in \mathbb{B} \quad \forall r \in R_h^-.$$
 (7c)

Model (7) presents a formulation for the ridesharing problem for route set R_h^- . Objective (7a) minimizes the total cost of the selected routes. Constraints (7b) ensure that every request is fulfilled by one of the routes. Integral route selections are enforced by Constraints (7c). Problem (7) can be seen as a special case of the problem solved by Auad and Van Hentenryck (2021).

The fleet-sizing optimization Given the optimal shuttle routes from Model (7), and the single passenger routes related to P_{direct} , the fleet-sizing algorithm finds the minimum number of shuttles necessary to cover these routes. The fleet-sizing model uses a graph $\mathcal{G} = (\mathcal{V}, \mathcal{A})$, where a vertex r corresponds to a route, and an arc (r, r') indicates that it is feasible for a shuttle to serve route r' after serving route r, i.e., the ending time of route r, plus the time to relocate to the start of route r', is before the starting time of route r'. The graph G is extended with a source and a sink, denoted by src and snk respectively. The arc set A is extended with arcs from the source to all other vertices and arcs from all other vertices to the sink.

$$\min \quad \sum_{a \in \delta^+(src)} f_a, \tag{8a}$$

s.t.
$$\sum_{a \in \delta^{-}(r)} f_{a} = \sum_{a \in \delta^{+}(r)} f_{a} \quad \forall r \in \mathcal{V} \setminus \{src, snk\},$$
 (8b)
$$\sum_{a \in \delta^{-}(r)} f_{a} = 1 \qquad \forall r \in \mathcal{V} \setminus \{src, snk\},$$
 (8c)
$$f_{a} \geq 0 \qquad \forall a \in \mathcal{A}.$$
 (8d)

$$\sum_{c \in S^{-}(s)} f_a = 1 \qquad \forall r \in \mathcal{V} \setminus \{src, snk\}, \tag{8c}$$

$$f_a \ge 0 \qquad \forall a \in \mathcal{A}.$$
 (8d)

Formulation (8) presents the fleet-sizing problem as a minimum flow problem with covering constraints. Let f_a be the flow over arc $a \in \mathcal{A}$, and define $\delta^-(r)$ and $\delta^+(r)$ to be the sets of arcs going into and out of vertex $r \in \mathcal{V}$ respectively. By definition, a unit flow from the source to the sink corresponds to a feasible schedule for a single shuttle. Therefore, Objective (8a) minimizes the size of the fleet by minimizing the total flow coming out of the source. Constraints (8b) and (8c) ensure that the flows are balanced and that every route is served. Note that continuous variables may be used, because the coefficient matrix is totally unimodular.

4.4 Real-time shuttle dispatching

To perform a realistic simulation of an ODMTS, it is necessary to consider how the system is operated in real time and, in particular, how to dispatch and route the shuttles. To this end, the Real-Time Dial-A-Ride System (RTDARS) by Riley et al. (2019) is embedded into the simulator to dynamically dispatch shuttle requests. The simulator provides the RTDARS with the current status of the shuttles in the fleet, and with shuttle requests based on the scenario demand. Requests are only passed on as they arrive in real time, to prevent unrealistic anticipation.

The RTDARS divides time into epochs of length l and performs two tasks for each period: it batches arriving shuttle requests during the epoch, and it solves an optimization problem to route and dispatch unserved requests from previous epochs. A high-level overview of the algorithm is presented here, and a more detailed description is provided by Riley et al. (2019). The objective of the static optimization problem at every epoch is to create minimum cost shuttle routes that serve the requests. These routes respect the shuttle capacity $Q^{shuttle}$ and ensure that passengers do not deviate too much from the shortest path. Additionally, there is the option to postpone requests to the next epoch by incurring a penalty. The cost c_r of route r is the sum of the waiting times before pickup. The cost of not serving request p is given by g_p , which increases exponentially based on how long the rider has been waiting. The initial penalty \bar{g} doubles every ten epochs to ensure that postponed requests are eventually served.

Let P be the set of unserved shuttle requests from previous epochs, let R_s be the set of routes that can be assigned to shuttle $s \in S$, and let $R = \bigcup_{s \in S} R_s$. Feasible shuttle routes respect previously committed actions, vehicle capacity, and a limit on the time deviation from the shortest path. The binary variable θ_r takes on the value one if and only if route $r \in R$ is part of the solution. For every request $p \in P$, variable w_p is equal to one if and only if the request remains unserved in the current epoch. The parameter b_p^r indicates that request $p \in P$ is contained in route $r \in R$. Formulation (9) presents the problem formulation.

min
$$\sum_{r \in R} c_r \theta_r + \sum_{p \in P} g_p w_p,$$
s.t.
$$\sum_{r \in R} b_p^r \theta_r + w_p = 1 \quad \forall p \in P,$$

$$\sum_{r \in R_s} \theta_r = 1 \quad \forall s \in S,$$
(9c)

s.t.
$$\sum_{r \in R} b_p^r \theta_r + w_p = 1 \quad \forall p \in P,$$
 (9b)

$$\sum_{r \in R_{+}} \theta_{r} = 1 \quad \forall s \in S, \tag{9c}$$

Table 2
The parameter values for the case study.

Parameter	Value		
L	4 h (time horizon 6 am-10 am)		
L^+	6 h (time horizon 6 am-12 pm)		
F^{bus}	{8, 12, 16} (two, three, or four buses per hour)		
F^{rail}	{24} (six per hour)		
$ V_H $	57 transit hubs (38 rail stations, 19 bus-only hubs)		
α	Time is valued at \$7.25 per hour (US federal minimum wage)		
τ_a	Shuttle and bus travel times from OpenStreetMap, rail from schedule		
d_a	Distances from OpenStreetMap		
cbus	\$72.15 per hour		
cshuttle	\$27.31 per hour		
$\bar{c}^{shuttle}$	\$1 per mile		
K	4 arcs (at most three transfers)		
ρ	Tolerance factor 1.5		
Δ	30 s		
$Q^{shuttle}$	4 passengers		
Q^{bus}	57 passengers		
Q^{rail}	576 passengers (192 for green line)		
1	30 s per epoch		
\bar{g}	420 s		

$$\theta_r \in \mathbb{B} \quad \forall r \in R,$$
 (9d)

$$w_p \in \mathbb{B} \quad \forall p \in P.$$
 (9e)

Objective (9a) minimizes the cost of the selected routes and the penalties incurred for leaving requests unserved. Constraints (9b) specify that every request must be served, or a penalty is incurred. Constraints (9c) ensure that every shuttle is assigned a single route. Eqs. (9d) and (9e) are the integrality conditions. Riley et al. (2019) solve the static optimization problem with column generation. This algorithm iteratively generates promising shuttle routes (columns) with disjoint sets of requests. After reaching a stopping condition (based on real-time requirements), Problem (9) is solved for a restricted route set that only contains the routes that have been generated.

4.5 Simulation

The RTDARS is embedded in the simulator of Riley et al. (2019) to evaluate the performance of the designed ODMTS. The network design is provided by the design problem, the number of shuttles is provided by the ridesharing and fleet-sizing algorithms, and the demand is defined by the scenario. Passenger trips are revealed over time, and at every time increment the simulator updates the position of every passenger and every vehicle. Results are obtained for time horizon L by simulating the extended horizon L^+ and truncating the results.

The original simulator only handled shuttle trips, and the following changes are made to simulate the ODMTS. For every incoming trip request, the optimal path through the network is determined as defined in Section 4.2. When a shuttle connection is encountered, a shuttle request is posted to the RTDARS, while for bus and rail connections, passengers take the first vehicle with an empty seat along their predetermined route. The vehicle capacities are given by $Q^{shuttle}$, Q^{bus} , and Q^{rail} . At the start of the time horizon, the shuttles are distributed over the hubs proportionally to the average demand in each area. The bus arcs in the design are grouped into lines, and each line is assigned the minimum number of buses necessary to obtain the chosen frequency. Buses are spaced out evenly, but the rail and bus schedules are not synchronized. Solving a scheduling problem may improve transfer times, and is an interesting direction for future work. If the results show that the RTDARS is overwhelmed and shuttle waiting times are long, then the fleet size is increased by 10% and the simulation is restarted. This increase is to compensate for the fact that the ridesharing and fleet-sizing optimizations assume perfect information, while the RTDARS receives requests dynamically.

The simulator allows for high-fidelity analyses of the ODMTS system. The analyses are based on simulated movements of riders and vehicles, not on the design assumptions. For example, the ODMTS design problem uses expected waiting times, where simulation results allow for calculating the actual waiting time for every rider.

5 Baseline ODMTS for Atlanta

This section presents a baseline ODMTS for the city of Atlanta to assess the resiliency of ODMTS during a pandemic. To provide the proper context, the baseline ODMTS is compared to the existing transit system in terms of service quality and cost.

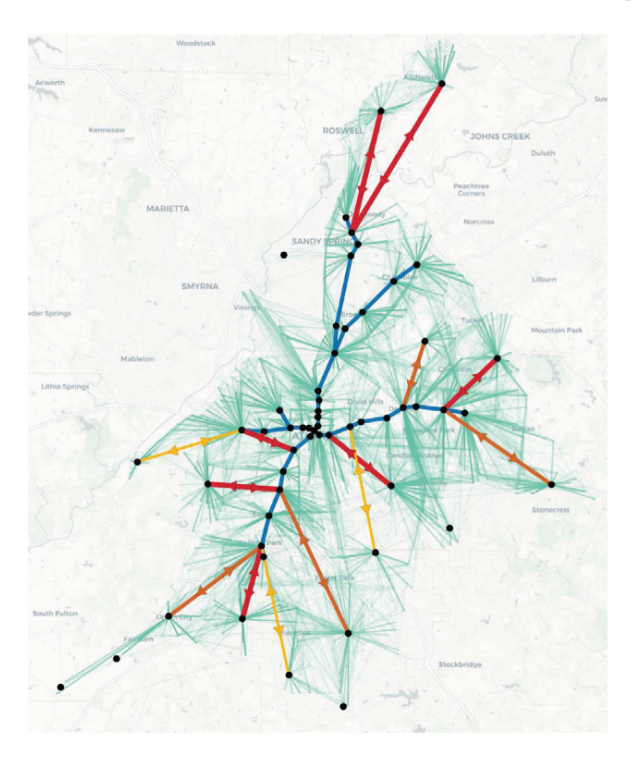


Fig. 9. The baseline ODMTS for Atlanta. (For interpretation of the references to color in this figure legend, the reader is referred to the web version of this article.)

Table 3Distribution of total waiting times per mode for trips using that mode (Baseline).

		Wait time (min)		
		0–5	5–10	>10
	Shuttle	57%	37%	6%
Baseline	Bus	45%	38%	18%
	Rail	63%	32%	5%

Settings Table 2 presents the parameter values used in the case study, using the 2018 data introduced in Section 3.1. Recall that the ODMTS is designed for the 6 am–10 am morning peak. The current rail system is fixed, with a frequency of six per hour to approximate the MARTA schedule closely. The 19 bus-only hubs are chosen by iteratively selecting a location that is at least four miles from the other hubs, and has the most passenger activity. Road travel times and distances were obtained from OpenStreetMap using the GraphHopper library (OpenStreetMap, 2020). Traffic congestion is not taken into account. Note however cities like San Francisco have dedicated lanes for transit vehicles. Moreover, shuttle connections are typically local and short, and therefore less affected by traffic. For practical reasons, stops within a 1500 ft radius are clustered, and 15,479 unique trips remain.

Network design The resulting ODMTS design is shown in Fig. 9. Shuttle connections are depicted as thin lines (green), rail connections as thick lines (blue), and bus connections as arrows ranging from light to dark (yellow to red) for low to high frequencies. The rail is obviously the core of the network. Buses are mostly used to expand the rail, providing connections to high-density areas that it cannot reached. This holds for all four cardinal directions, and especially for the North. Other bus lines cover the Northeast, the Southeast, and the Southwest. The Northwest is served by shuttles, because most riders are close to the rail. The ridesharing and fleet-sizing optimizations estimate that 917 shuttles are necessary to operate the ODMTS. This number was scaled up by 20% to 1100 shuttles to obtain an acceptable service level. The bus service is provided by 24 buses.

Passenger convenience In real-time simulations, the average trip duration was found to be 25 min, with 18 min of travel and 7 min of waiting time. Rail-only riders (56%) spend 23 min in transit, which is similar to the estimate for the current system. For the remaining trips (44%), the trip duration is only 27 min for the ODMTS compared to 46 min for the current system. Table 3 shows the distribution of the waiting times over the different modes. Only 6% of the trips including a shuttle leg requires waiting more than 10 min for a shuttle. The bus and rail distributions provide a similar picture: waiting under five minutes is most common, and waiting longer than 10 min is least likely. Shuttle waiting times vary over time, while bus and rail waiting times are fairly constant. Fig. 10 shows that the average waiting time is about 6 min for a bus and 4 min for a train leg. The shuttle waiting times have a peak of about 6.5 min between 7am and 8am, which is the period that sees the most passengers. Around 6am, waiting times are also relatively long while the shuttles spread out over the region. After 8am, the shuttle waiting time rapidly decreases to only 3 min.

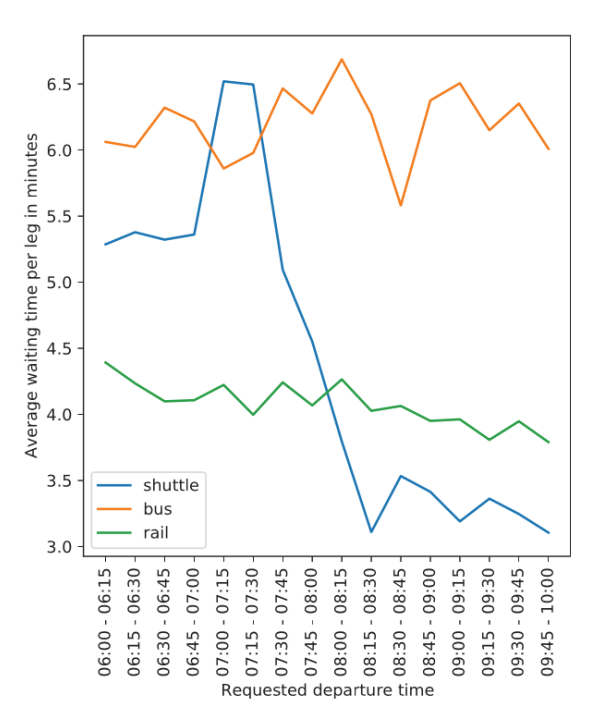


Fig. 10. Average waiting time per leg type over time.

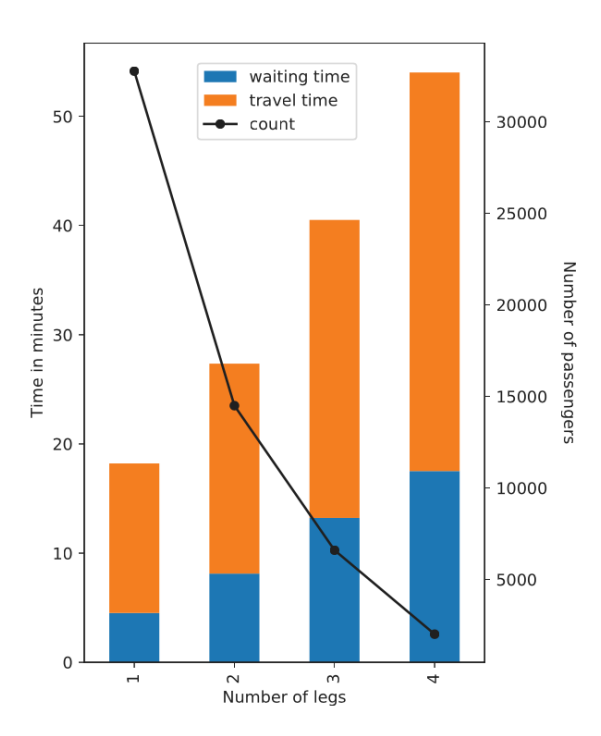


Fig. 11. Average passenger wait and travel times (left axis) and total trip counts (right axis) for a given number of legs per trip.

Fig. 11 shows how waiting times are distributed over the trips. Short trips have short waiting times, and waiting times increase almost proportionally with the length of the trip, which indicates a fair distribution. Furthermore, the counts show that trips with many transfers are rare: the vast majority of riders are served either by a direct trip or with a single transfer.

Capacity utilization It is interesting to report capacity utilization results, since social distancing measures will reduce capacity. The average utilization of buses and rail stays under 32% over the time horizon. The line chart in Fig. 12 shows the fraction of active shuttles over the time horizon. Almost all shuttles are active during the busiest period from 7am to 8am, but the waiting times show that the system is not overwhelmed. The same figure presents the total mileage for a given shuttle occupancy. It shows that riders can be offered individual shuttle rides most of the time, and that the amount of sharing increases when more shuttles are busy. The

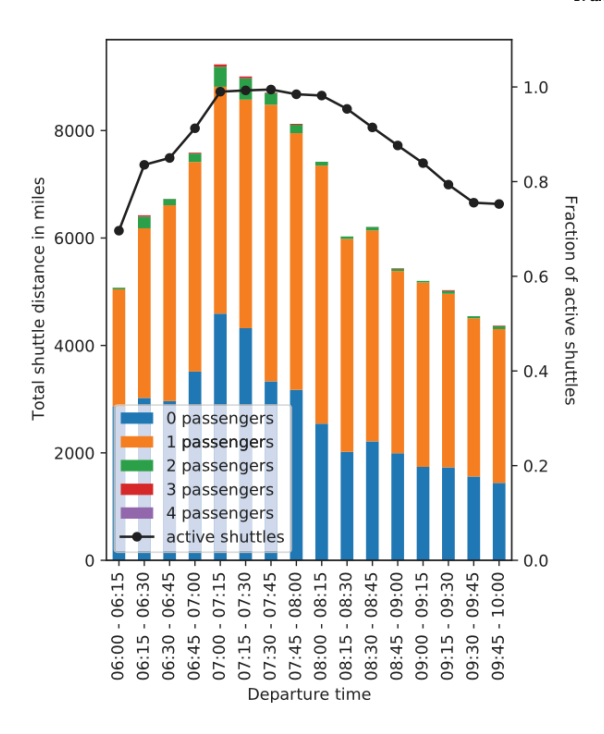


Fig. 12. Total miles driven at given occupancy (left axis) and fraction of shuttles active over time (right axis).

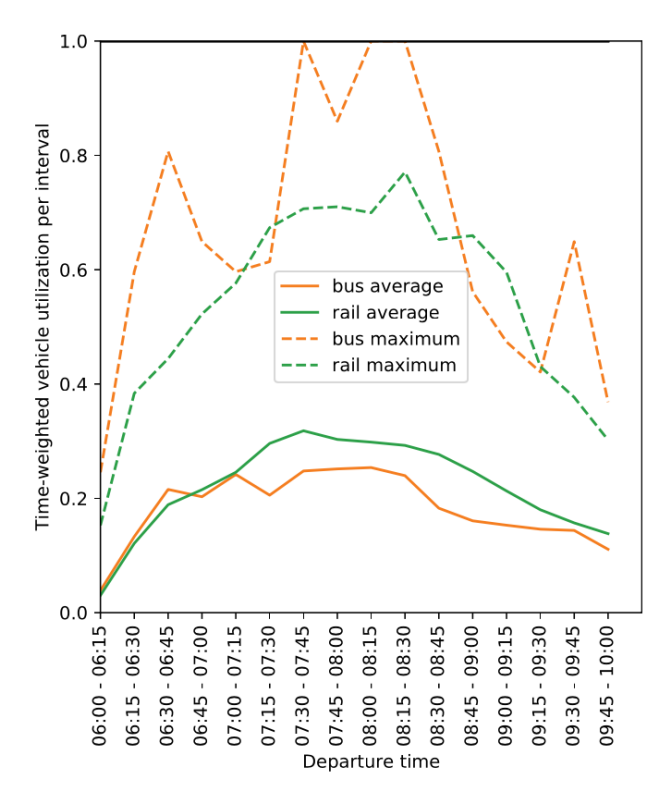


Fig. 13. Utilization of the buses and trains over time (Baseline).

low occupancy suggests that reducing shuttle capacity in a pandemic is feasible. In total, the shuttles drive 105,127 miles between 6am and 10am, which amounts to 96 miles per shuttle on average. Trains are never at capacity, and only 0.7% of bus passengers incur a delay due to buses being full. Fig. 13 provides additional details.

Road usage and congestion Fig. 14 visualizes the impact of the baseline ODMTS on the road network, where the opacity of each road increases with the number of times it is used by buses and shuttles. The figure shows that the ODMTS performs as intended, with

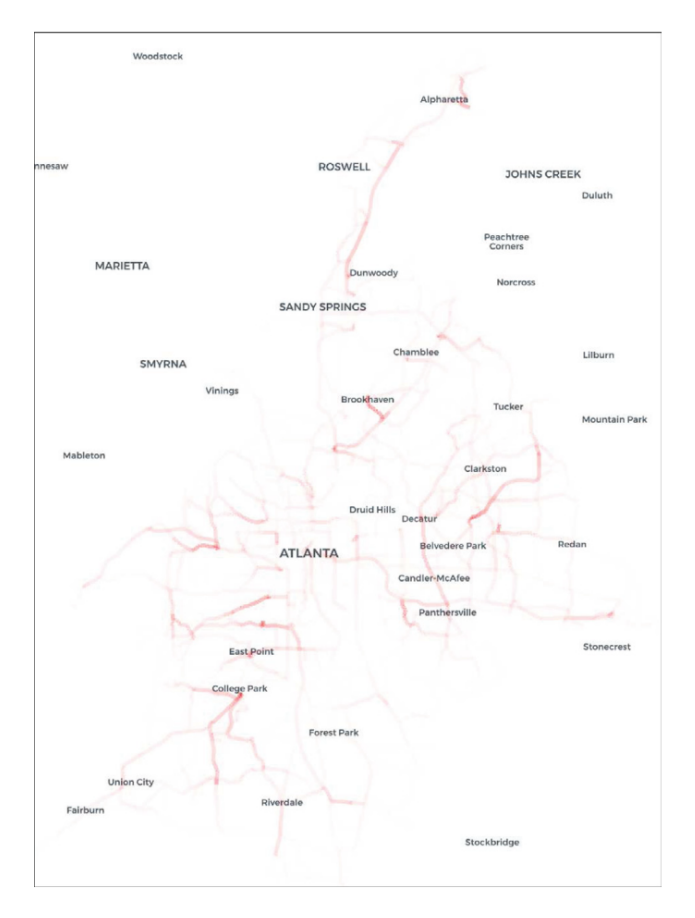


Fig. 14. Road usage with the ODMTS.

mainly local shuttle trips. The shuttle trips impose little traffic pressure on the main roads, which are served by a relatively small number of buses. Hence, by providing a convenient and accessible alternative to driving a car, ODMTS can also help to reduce congestion. For comparison, Fig. 15 visualizes the road usage when the same travelers would drive their personal vehicles. The figure suggests that if more people would switch from car to ODMTS, this could significantly reduce traffic, and especially relieve congestion on the main roads, which are most affected. Some roads (for instance) close to the College Park train station may seem to have additional traffic. Fig. 16 provides a close-up of this region. In fact, the ODMTS generates at most an average of 3.5 cars per minute more (red roads). The ODMTS also reduces the number of cars by up to 12.1 cars per minute compared to personal vehicles (blue roads).

Comparison with the current system To provide proper context, the baseline ODMTS is compared to the current system in terms of estimated cost and service quality. While this paper focuses on the resiliency of ODMTS, a more detailed comparison between the two systems is an interesting direction for future research. The estimated cost for buses in the morning peak is \$134k per day for the current system. For the baseline ODMTS, it is only \$127k for buses and shuttles together. These costs are calculated based on the hourly vehicle costs. Lower costs stem from the relatively low cost of operating shuttles compared to buses: The ODMTS only uses buses for busy corridors, where high-capacity vehicles are most efficient. For rail-only passengers, there is no significant difference between the systems obviously, but it is not known how these riders travel to the rail station. For current bus users, the ODMTS seems strongly preferred, as the trip duration is 19 min shorter on average. Other advantages of the ODMTS include better access to the public transit system, and less time for riders to get to a stop, as the on-demand shuttles can pick them up close to their origins.

Importance of buses As mentioned earlier, the core of the ODMTS for Atlanta is the rail network, and bus lines provide access to the rail for high-density areas. Shuttles, however, can perform the same task. This gives rise to the question of whether buses are important to the baseline ODMTS. The baseline ODMTS has 24 buses and 1100 shuttles. If buses are removed from the system, the ridesharing and fleet sizing algorithms indicate that 151 additional shuttles are necessary, for a total fleet of 1251 shuttles. The cost for the morning peak would then increase by 7.5% from \$127k to \$137k, which exceeds the cost of the current system of \$134k. This is consistent with the case study of ODMTS in Ann Arbor, where buses were shown critical (Basciftci and Van Hentenryck, 2020).

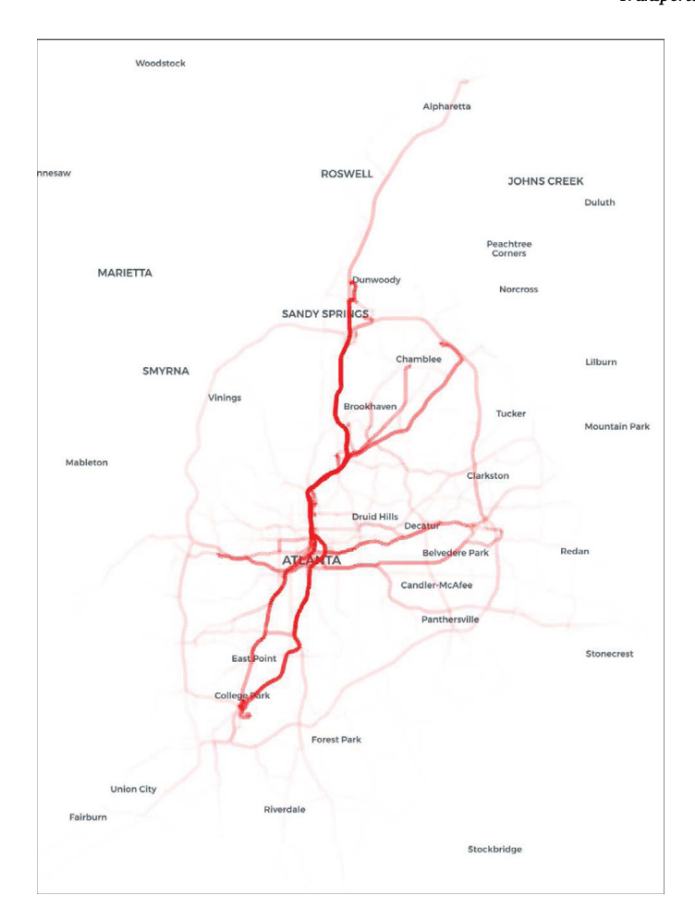


Fig. 15. Road usage without the ODMTS.

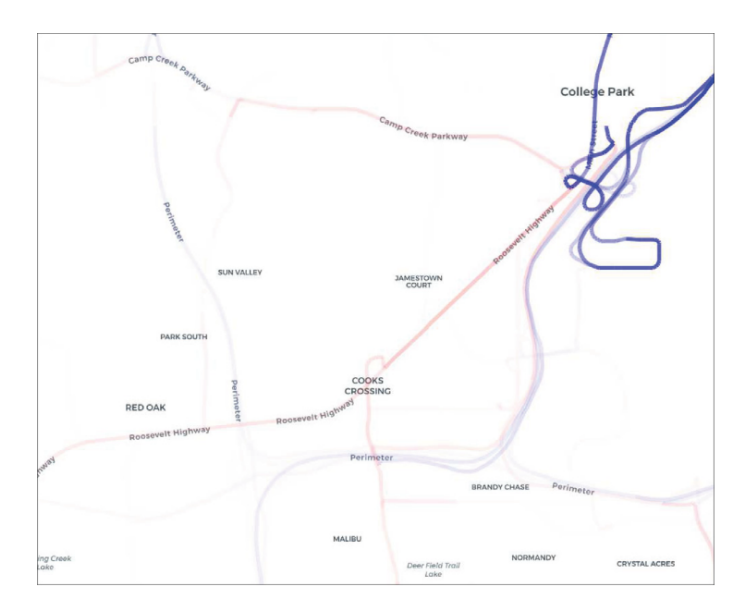


Fig. 16. Change in road usage around College Park due to the ODMTS (blue for improvement). (For interpretation of the references to color in this figure legend, the reader is referred to the web version of this article.)

6 Resiliency of ODMTS

The resiliency of the ODMTS during a pandemic is evaluated with scenarios that correspond to different periods of the COVID-19 pandemic. These scenarios differ in the level of ridership, and the amount of social distancing measures. The resiliency is assessed by investigating how the performance and cost evolve when the baseline design is kept in place and only the number of shuttles

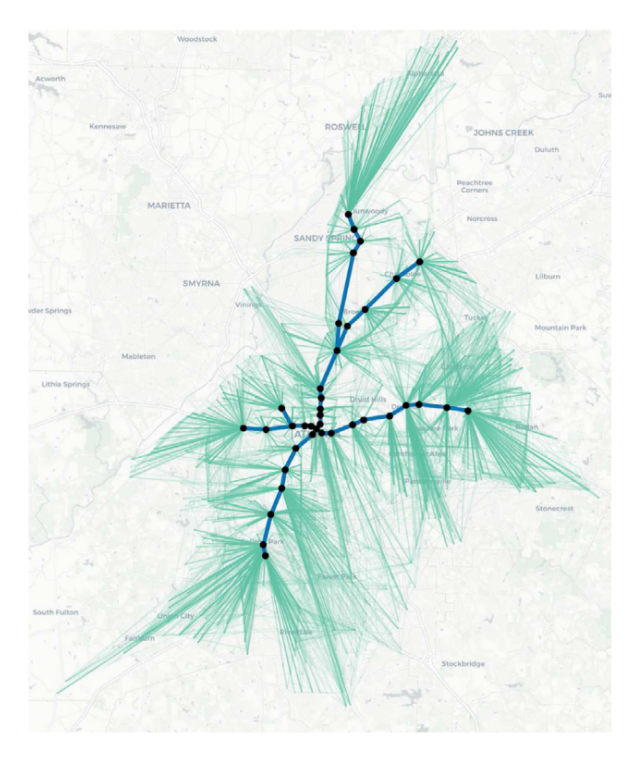


Fig. 17. The ODMTS for Atlanta without buses.

Table 4
Overview of scenarios settings and shuttle fleets.

Scenario name	Ridership level	Passengers	Capacity			Shuttle fleet	Shuttle fleet		
			Shuttle	Bus	Rail	Fixed design	Redesign	Budget	
Baseline	2018	55 871 (100%)	4	100%	100%	1100		\$127k	
Early Pandemic	March 2020	25 042 (45%)	1	50%	50%	846	837	\$106k	
Late Pandemic	April 2020	13 479 (24%)	1	50%	50%	510	514	\$98k	
Strict Late Pandemic	April 2020	13479 (24%)	1	0%	25%	602 ^a	599	\$98k	

^aBus subsystem removed from the design.

is scaled down. This is complemented by an evaluation that redesigns the network to take into account the change in demand and additional cleaning costs. Keeping the baseline ODMTS simplifies operations but a redesign may yield additional cost savings. For MARTA, only 33% of the operating expenses come from fare revenues, but this number may be significantly higher for other transit agencies. This section also studies how service levels change when this percentage increases.

6.1 Scenarios

Table 4 summarizes the scenarios used in the case study. The first scenario is the baseline, and the other three are pandemic scenarios with depressed demand and reduced vehicle capacities to allow for social distancing. Fleet sizes are provided by the ridesharing and fleet-sizing algorithms. The "Fixed design" column assumes that the baseline network design is kept in place for all scenarios, except for the strict late pandemic scenario, which removes the bus subsystem (see Fig. 17). For the "Redesign" column, the network is redesigned based on the scenario, and the fleet size is determined for the redesigned network (Section 6.3).

The passenger trips in the pandemic scenarios are sampled from the 2018 data until the ridership matches the pandemic level. Sampling is used because the trips observed during the pandemic are shaped by the essential service plan, and do not necessarily represent the actual demand. The early pandemic scenario is based on the ridership level around March 18th, 2020, with 70k bus and 60k rail transactions per day. The late pandemic scenarios use the April 2020 level with 40k bus and 35k rail transactions. Due to the lack of bus transaction data for April, the proportion of bus to rail trips is kept the same for April and scaled down based on number of rail trips. The bus and rail capacities are indicated as percentages of the total baseline capacity. A 50% capacity allows for only using every other seat for social distancing. As social distancing is difficult in a shuttle, only one passenger is allowed during the pandemic. The strict late pandemic scenario imposes even stricter measures: Buses are considered not safe, and the system operates with only single passenger shuttles and trains at 25% capacity.

Table 5
Statistics per scenario under the fixed design.

	Average trip duration (min)		Max. use of	Max. use of total capacity		Cost (\$)	
	Rail-only	Other	Bus	Rail		Ex. Clean.	Incl. Clean.
Baseline	23	27	25%	32%	127k	127k	127k
Early pandemic	22	26	17%	13%	106k	99k	105k
Late pandemic	22	26	10%	7%	98k	63k	66k
Strict late pandemic	22	25	0%	7%	98k	66k	70k

Table 6
Distribution of total waiting times per mode for trips using that mode.

		Wait time (min)			
		0–5	5–10	>10	
	Shuttle	57%	37%	6%	
Baseline	Bus	45%	38%	18%	
	Rail	63%	32%	5%	
	Shuttle	62%	35%	4%	
Early pandemic	Bus	44%	36%	20%	
	Rail	64%	31%	5%	
	Shuttle	62%	35%	4%	
Late pandemic	Bus	44%	39%	17%	
-	Rail	64%	31%	5%	
	Shuttle	53%	37%	10%	
Strict late pandemic	Bus	n.a.	n.a.	n.a.	
	Rail	61%	33%	6%	

One interesting observation is that for all pandemic scenarios, the number of shuttles is smaller than that for the baseline scenario. It is not obvious that this would be the case, and it demonstrates that ridership decreases sufficiently to allow for both a reduction in capacity *and* a reduction in the number of shuttles. It follows that the baseline fleet is sufficiently large to operate the system during a pandemic, and no additional vehicles are necessary.

Every scenario is assigned a budget for buses and shuttles that takes into account that reduced ridership affects fare revenue. For the current system, 33% of the operating expenses are paid from fares and direct revenue, while capital expenditures are completely funded from other sources. The baseline budget is taken to be the normal cost of the system, 92% of which is operating expenses (labor and maintenance) and 8% is capital expenditures (depreciation). For the other scenarios, the budget is reduced proportionally to the change in available funds. For the early pandemic scenario, for example, the number of passengers is reduced by 55%. This results in a reduction of operating funds by 18%, and therefore a reduction of the budget by 17% to \$106k.

6.2 Resiliency under fixed design

This section evaluates the ODMTS resiliency when the baseline network design stays in place during the pandemic. Table 5 presents the aggregate results. The average trip durations suggest that the ODMTS is very resilient in terms of rider convenience. For riders not using rail, the average trip duration remains under 27 min on average. These results are also valid for individual trips. Table 6 shows that, for the early and late pandemic scenarios, the wait times are comparable to the baseline in distribution. In the strict late pandemic scenario, waiting times for the shuttles go up, as a result of removing the buses.

Fig. 18 displays the waiting times over time for the strict late pandemic scenario. The pattern is similar to the baseline, except that the shuttle waiting times are slightly larger. But, even during the peak, the average waiting time for a shuttle leg is at an acceptable 6.5 min. This shows that a high quality of service can be provided, even if buses are no longer used, at the cost of increasing the number of shuttles from 510 to 602.

In the baseline scenario, the capacity of the buses and the trains is not restrictive, and this still holds true for the pandemic scenarios. Table 5 shows that the average bus utilization does not exceed 17%, while 50% of capacity is available. The average train utilization does not exceed 13% in any pandemic scenario. This allows for additional social distancing, and it provides opportunities for taking some vehicles out of the rotation and cleaning them during the day, without creating capacity shortages. A simulation of the early pandemic scenario confirms that halving the rail frequency would double the rail waiting time and the train utilization as expected, but does not otherwise affect the system. This also suggests that there is an opportunity to save costs during a pandemic by modifying the rail system. This is studied for traditional systems by Gkiotsalitis and Cats (2021a), for example, and is also an interesting direction for future research in the context of ODMTS. Fig. 19 evaluates the utilization of the shuttles during the pandemic. For each pandemic scenario, it shows the number of active shuttles during the day, compared to the available number. For all scenarios, the number of shuttles is sufficient, and most of the shuttles are being used during the peak from 7am to 8am.

While the performance of the ODMTS is similar for all scenarios, it should be verified that the system remains affordable. The budget and cost columns in Table 5 compare the cost of the system to the reduced budget that results from decreased fare revenues.

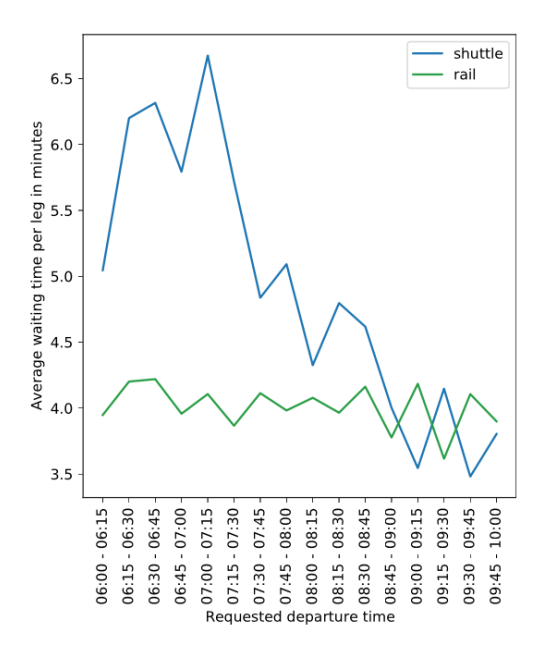


Fig. 18. Average waiting time over time for a leg of a given mode (Strict late pandemic).

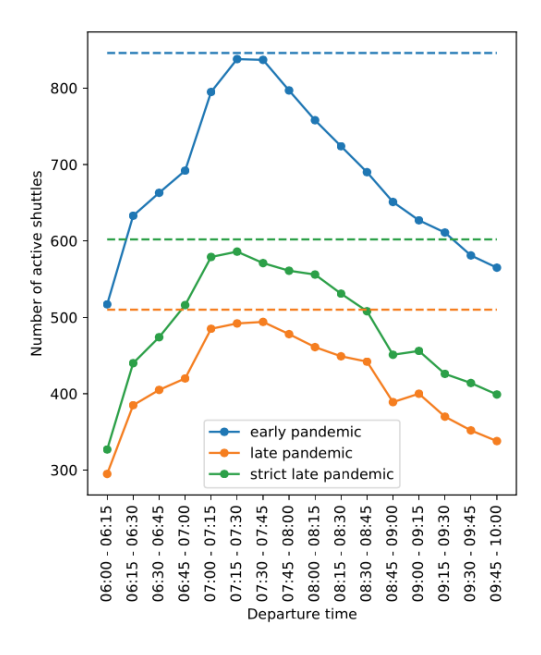


Fig. 19. Number of shuttles active over time for different pandemic scenarios (Number available as dashed line).

The cost is reported both with and without additional cleaning cost for sanitizing and disinfecting the fleet during the COVID-19 pandemic. The cleaning cost is estimated at \$3.37 per hour for buses, and \$1.69 per hour for shuttles (see the Appendix). For the early pandemic scenario, the cost of the system (\$99k excl., \$105k incl.) stays within the \$106k budget, even when COVID-19 fleet sanitation is included. This suggests that operating the ODMTS at the same service level during this stage of the pandemic is economically viable. Section 6.4 explores how the quality of service is affected when a smaller budget is enforced. For the late and strict late pandemic scenarios, the budget far exceeds the cost.

The resiliency of ODMTS for a fixed network design stems from the flexibility of the on-demand shuttles: Scaling the number of shuttles appropriately can compensate for large changes in demand and reductions in capacity, without exceeding the budget. ODMTS differs in this respect from traditional systems, for which providing the same level of service within a reduced budget is often impossible.

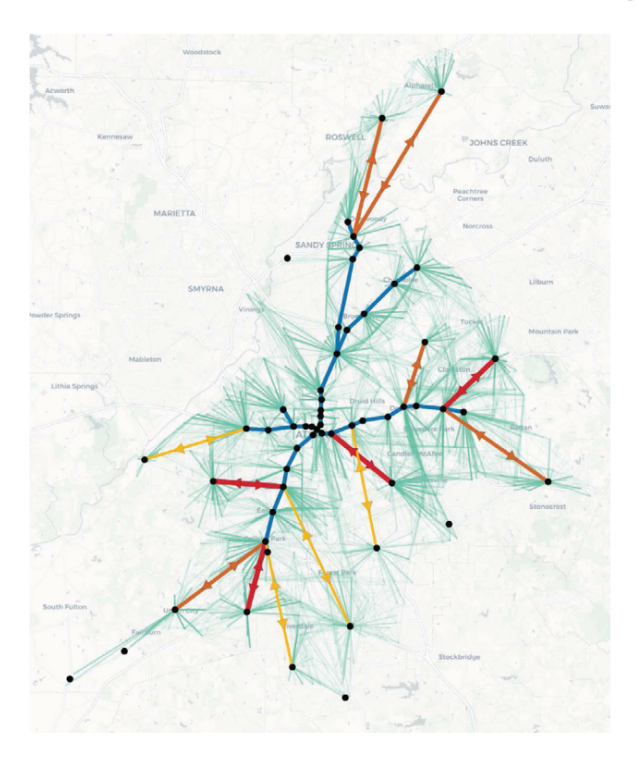


Fig. 20. ODMTS redesign for early pandemic ridership.

6.3 Resiliency under redesign

This section considers the cases where the transit agency redesigns the network to better fit the pandemic circumstances and obtain additional savings, especially if the transit system is expected to be affected for a longer period of time. For each pandemic scenario, the ODMTS design problem is solved for the respective pandemic ridership level. To account for cleaning and social distancing, the bus cost per hour c^{bus} is increased by \$3.37, and the shuttle cost per mile $\bar{c}^{shuttle}$ is replaced by the actual cost (incl. cleaning) obtained from the simulations under fixed design. Figs. 20 and 21 present the networks for the early and late pandemic ridership levels respectively.

As ridership decreases, some of the bus lines are closed, and others are reduced in frequency. The number of buses is reduced from 24 in the baseline design to 21 in the early pandemic scenario and 13 for the late pandemic scenario. Due to the relatively high cost of shuttles during a pandemic, the redesigns maintain relatively large bus subsystems compared to their demand. Passengers are assigned fewer direct shuttle trips, which allows the shuttle fleet to stay roughly the same size, despite the smaller number of buses. Compared to the fixed design, the redesigned network in the early pandemic scenario decreases the number of direct shuttle trips by 7.8% and increases peak average bus utilization from 17% to 20%. For the late pandemic scenario, direct shuttle trips decrease by 6.3%, while bus utilization increases from 10% to 18%.

Redesigning the network results in \$2.0k (1.9%) savings for the early pandemic scenario, and \$2.9k (4.3%) savings for the late pandemic scenario. In terms of performance, the average trip duration is increased by less than a minute. This is possible because the smaller networks fit better with the reduced demand, and passengers make less use of shuttles, which are more expensive during the pandemic due to cleaning cost and social distancing.

Redesigning the network based on the scenario may lead to additional cost savings, without compromising performance. This comes at the cost of a more intensive use of buses, and slightly longer waiting times for passengers using the bus subsystem. The cost savings are more significant in the late pandemic scenario, where ridership is more depressed. The increase in average bus wait time is under 2.5 min.

The possibility to redesign the network gives the ODMTS additional flexibility to deal with unexpected changes in demand, on top of the flexibility provided by the on-demand shuttles. Rather than changing the design over time, the network design model may also be generalized to create a single fixed design with good performance in expectation. This is an interesting direction for future research, but would require predicting the path of the pandemic, which has been very difficult for COVID-19.

6.4 Larger budget reductions

Section 6.2 showed that, in the early pandemic scenario, the cost of operating the ODMTS is within the reduced budget. This conclusion is critically dependent on how ridership affects the budget. In Atlanta, fares and direct revenues cover 33% of the operating expenses, but this number may be higher in other areas. In New York City, for example, the share is 55%, and in the San

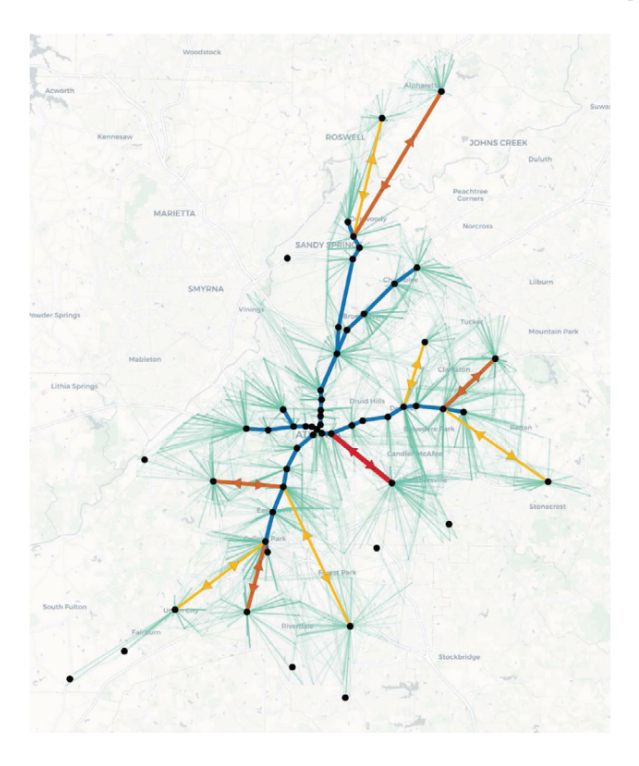


Fig. 21. ODMTS redesign for late pandemic ridership.

Francisco Bay Area it is even 70% (Federal Transit Administration, 2018). In these cases, loss of ridership has a larger impact on the budget, and operating with the proposed number of shuttles is no longer feasible.

To study the effect of larger budget reductions, two variations of the early pandemic scenario are considered: one where fare revenues cover 50% of the operating expenses, which corresponds to doubling the current ticket price, and one where the share is doubled to 66%. As a result, the budget is reduced from \$106k to \$95k and \$84k respectively. Even using the redesigned network, the reduced budgets do not allow for operating 837 shuttles, as determined by the ridesharing and fleet-sizing algorithms. Instead, the number of shuttles is reduced to 763 and 671 respectively, to fit the budget, including additional costs for cleaning. Fig. 22 shows how shuttle utilization is impacted by reducing the number of shuttles. In the 33% case, most shuttles are used during the 7am to 8am peak, but there are always shuttles available for incoming requests. When the number of shuttles is reduced to 763, almost all shuttles are active at the same time for about an hour. The system does not seem to be overwhelmed, however, as the number of active shuttles decreases quickly after the peak. The 66% case paints a different picture: to operate the system with only 671 shuttles, the fleet is completely occupied for about two hours to keep up with incoming requests.

When the fleet is busy, this affects the shuttle waiting time. Fig. 23 compares the waiting times for a shuttle leg under the different budgets. It can be seen that reducing the budget results in a higher peak in shuttle waiting times. Furthermore, the peak is wider at lower budgets, corresponding to the busy periods in Fig. 22. Reducing the number of shuttles from 837 (33% case) to 763 (50% case) only has a minor impact on performance. The waiting time for a shuttle leg increases by less than one minute during the peak, and the average trip duration for all passengers remains practically the same. Going down to 671 shuttles (66% case) presents a more significant trade-off between cost and convenience. The impact on the average trip duration is only two minutes, but the average shuttle leg waiting time goes up to 13 min during the peak. It is up to the transit agency to decide whether this wait is acceptable during a pandemic, given that it allows for operating the system within a very restrictive budget that also covers additional cleaning, without compromising access to public transit.

7 Conclusions

This paper studied the resiliency of ODMTS during a pandemic, which comes with depressed ridership and revenues, and increased safety requirements. Operating in this environment is a challenge for public transit agencies, which are forced to cut routes, reduce service hours, or lower the service frequency. An ODMTS can respond to a pandemic by scaling down the number of shuttles as needed. However, it was an open issue whether, under such conditions, the ODMTS can still provide accessible public transit with a high quality of service that stays within the more restricted budget. To answer this question, the paper presented an ODMTS optimization pipeline which was applied to a variety of pandemic scenarios and evaluated using a high-fidelity simulator.

The case study considered the transit system for the city of Atlanta based on actual data and observations from the COVID-19 pandemic. The starting point was a baseline ODMTS designed under regular, non-pandemic circumstances. During a pandemic, the rail and bus schedules may be kept the same, while the number of shuttles is scaled down. It was shown that this allows the ODMTS

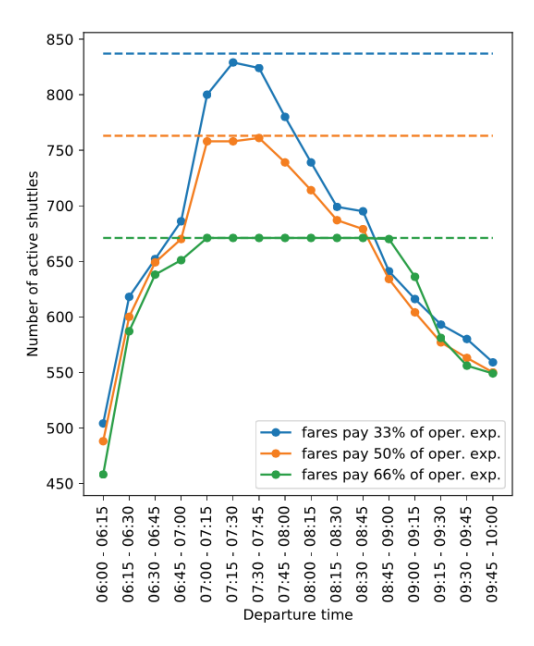


Fig. 22. Number of shuttles active over time for the early pandemic scenario for different budgets (Number available as dashed line).

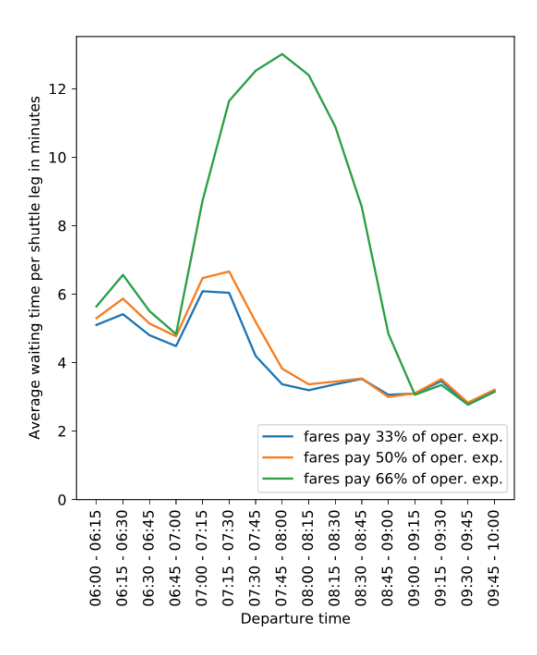


Fig. 23. Average shuttle waiting time over time for different budgets.

to provide almost identical performance during a pandemic. Furthermore, the cost of the system decreases sufficiently to make up for lost revenues. Transit agencies may also decide to redesign the network during a pandemic to better fit the reduced demand. The results showed that this allows for additional cost savings without compromising service quality, and this benefit is more significant when demand is more depressed. Finally, operating the ODMTS under a stricter budget was considered to account for the realities of other transit systems. The simulations showed a trade-off between the budget and the peak shuttle waiting times, but overall the average waiting time is not much affected.

The case study results suggest that ODMTS provide significant resiliency during pandemic response. Furthermore, it supports earlier findings that combining on-demand shuttles with high-frequency buses and trains may provide a cost-efficient alternative to traditional public transit systems.

CRediT authorship contribution statement

Ramon Auad: Methodology, Software, Validation, Formal analysis, Investigation, Writing – original draft. Kevin Dalmeijer: Conceptualization, Methodology, Software, Validation, Formal analysis, Investigation, Writing – original draft. Connor Riley:

Methodology, Software, Validation, Formal analysis, Investigation, Writing – original draft. **Tejas Santanam:** Software, Validation, Formal analysis, Investigation, Writing – original draft. **Anthony Trasatti:** Methodology, Software, Validation, Formal analysis, Investigation, Writing – original draft. **Pascal Van Hentenryck:** Conceptualization, Methodology, Validation, Formal analysis, Investigation, Data curation, Writing – review & editing, Supervision, Project administration, Funding acquisition. **Hanyu Zhang:** Software, Validation, Formal analysis, Investigation, Writing – original draft.

Acknowledgments

This research is partly supported by NSF Leap HI proposal NSF-1854684 and Department of Energy Research Award 7F-30154.

Appendix. Cost calculations

To compare the cost of the current system to that of an ODMTS, it is necessary to estimate the cost of operating a bus compared to operating an on-demand shuttle. MARTA reports that the operating expenses for buses are \$104.10 per vehicle revenue hour. However, this number includes expenses for general administration and facility maintenance, and excludes depreciation of the vehicles. To present a fair comparison, it is assumed that buses and shuttles only differ in labor cost, vehicle maintenance cost, and vehicle depreciation. In particular, the cost of fuel and lubricants is ignored, as this is a relatively small component of the cost. If it were to be included, this would favor shuttles due to their better fuel efficiency.

The cost of one person-hour of operating a bus is \$23.52 in salaries and wages, to which \$16.03 (68%) is added in fringe benefits (Federal Transit Administration, 2018). It is assumed that one vehicle revenue hour requires one person-hour of labor, which results in a conservative labor cost estimate. The maintenance cost is estimated at \$19.17 per vehicle revenue hour. This number results from adding up salaries and wages, fringe benefits, and materials in the 'vehicle maintenance' category, and dividing by the number of vehicle revenue hours. The majority of the MARTA fleet consists of 40-foot compressed natural gas buses with a current purchase price of \$625k (Federal Transit Administration, 2018; Dickens, 2020). These buses have a useful life benchmark of 12 years, and are used for 3878 vehicle revenue hours per year on average. This corresponds to a \$13.43 depreciation per revenue hour.

For the purpose of comparing buses to shuttles, this brings the cost of a bus to \$72.15 per hour. MARTA operates 465 buses in maximum service (Federal Transit Administration, 2018), which corresponds to \$134k during the morning peak.

It is assumed that shuttle drivers are paid the average wage of a bus driver in Atlanta and that they receive the same 68% of fringe benefits. This amounts to \$14.42 per hour in wages (Glassdoor, 2020) and \$9.83 in fringe benefits, for a total labor cost of \$24.25 per hour. The maintenance cost is estimated at \$0.09 per mile for a medium sedan (American Automobile Association, 2019), which results in \$1.13 per hour, assuming that shuttles and buses are used for the same number of hours per day and have the same daily mileage on average. For the depreciation cost, it is assumed that shuttles have a purchase price of \$30k and are replaced every four years, which is after 191k miles. This leads to a \$1.93 depreciation cost per hour. Adding up these numbers, the comparable total cost of a shuttle is \$27.31 per vehicle revenue hour.

From an economic perspective, the public transit agencies may aim to recruit ridesharing drivers instead of bus drivers for operating the shuttles. According to the Ridester's Driver Earnings Survey, the average Uber driver in the US earns \$19.36 per hour (Helling, 2020). The car is the driver's property, and the driver is responsible for the associated costs. Based on the maintenance and depreciation costs as above, this results in an effective hourly wage of under \$16.30, which is low compared to \$24.25 for a bus driver.

The additional cost for sanitizing and disinfecting vehicles during COVID-19 is estimated from data provided by Gwinnett County Transit, the public transit system in the neighboring county of Gwinnett. The data spans March to November 2020. The average cost per operating hour is calculated by dividing the total cost of fleet sanitation by the number of bus operating hours, which results in a cost of \$3.37 per hour. This paper assumes that cleaning significantly smaller on-demand shuttles is possible for half that cost, that is, \$1.69 per hour.

References

Agatz, N., Hewitt, M., Thomas, B.W., 2021. "Make no little plans": Impactful research to solve the next generation of transportation problems. Networks 77, 269–286. http://dx.doi.org/10.1002/net.22002.

American Automobile Association, 2019. Your driving costs. https://exchange.aaa.com/automotive/driving-costs/.

Atlanta Regional Commission, 2019. Population (by census tract) 2018. https://opendata.atlantaregional.com/datasets/population-by-census-tract-2018. Atlanta Regional Commission, 2020. How COVID-19 has Affected Transportation in Metro Atlanta. ARC Webinar.

Auad, R., Van Hentenryck, P., 2021. Ridesharing and fleet sizing for on-demand multimodal transit systems. arXiv:2101.10981.

Barry, J.J., Newhouser, R., Rahbee, A., Sayeda, S., 2002. Origin and destination estimation in New York City with automated fare system data. Transp. Res. Rec. 1817 (1), 183–187. http://dx.doi.org/10.3141/1817-24.

Basciftci, B., Van Hentenryck, P., 2020. Bilevel optimization for on-demand multimodal transit systems. In: Hebrard, E., Musliu, N. (Eds.), Integration of Constraint Programming, Artificial Intelligence, and Operations Research. Springer, pp. 52–68. http://dx.doi.org/10.1007/978-3-030-58942-4_4.

Basciftci, B., Van Hentenryck, P., 2021. Capturing travel mode adoption in designing on-demand multimodal transit systems. arXiv:2101.01056.

Benders, J.F., 1962. Partitioning procedures for solving mixed-variables programming problems. Numer. Math. 4, 238–252. http://dx.doi.org/10.1007/BF01386316.

Boland, N., Hewitt, M., Marshall, L., Savelsbergh, M., 2017. The continuous-time service network design problem. Oper. Res. 65 (5), 1303–1321. http://dx.doi.org/10.1287/opre.2017.1624.

Codato, G., Fischetti, M., 2006. Combinatorial Benders' cuts for mixed-integer linear programming. Oper. Res. 54 (4), 756–766. http://dx.doi.org/10.1287/opre. 1060.0286.

Dalmeijer, K., Van Hentenryck, P., 2020. Transfer-expanded graphs for on-demand multimodal transit systems. In: Hebrard, E., Musliu, N. (Eds.), Integration of Constraint Programming, Artificial Intelligence, and Operations Research. Springer, pp. 167–175. http://dx.doi.org/10.1007/978-3-030-58942-4_11.

Dezső, B., Jüttner, A., Kovács, P., 2011. LEMON – an open source C++ graph template library. Electron. Notes Theor. Comput. Sci. 264 (5), 23–45. http://dx.doi.org/10.1016/j.entcs.2011.06.003.

Dickens, M., 2020. Public Transportation Vehicle Database. American Public Transportation Association.

Federal Transit Administration, 2018. National transit database.

Gkiotsalitis, K., Cats, O., 2021a. Optimal frequency setting of metro services in the age of COVID-19 distancing measures. Transportmetrica A. http://dx.doi.org/10.1080/23249935.2021.1896593.

Gkiotsalitis, K., Cats, O., 2021b. Public transport planning adaption under the COVID-19 pandemic crisis: literature review of research needs and directions. Transp. Rev. 41 (3), 374–392. http://dx.doi.org/10.1080/01441647.2020.1857886.

Glassdoor, 2020. Bus driver salaries in Atlanta, GA Area. https://www.glassdoor.com/Salaries/atlanta-bus-driver-salary-SRCH_IL.0,7_IM52_KO8,18.htm. Accessed: 2020-10-22.

Goldbaum, C., Wright, W., 2020. 'Existential Peril': Mass Transit Faces Huge Service Cuts Across U.S.. The New York Times.

Gouveia, L., Leitner, M., Ruthmair, M., 2019. Layered graph approaches for combinatorial optimization problems. Comput. Oper. Res. 102, 22–38. http://dx.doi.org/10.1016/j.cor.2018.09.007.

Helling, B., 2020. Ridester's 2020 Independent Driver Earnings Survey - Driver Income Revealed. Ridester.

Laporte, G., Louveaux, F.V., Van Hamme, L., 2002. An integer L-shaped algorithm for the capacitated vehicle routing problem with stochastic demands. Oper. Res. 50 (3), 415–423. http://dx.doi.org/10.1287/opre.50.3.415.7751.

Liu, L., Miller, H.J., Scheff, J., 2020. The impacts of COVID-19 pandemic on public transit demand in the United States. PLOS ONE 15 (11), 1–22. http://dx.doi.org/10.1371/journal.pone.0242476.

Mahéo, A., Kilby, P., Van Hentenryck, P., 2019. Benders decomposition for the design of a hub and shuttle public transit system. Transp. Sci. 53 (1), 77–88. http://dx.doi.org/10.1287/trsc.2017.0756.

MARTA, 2020. Train stations & schedules. https://www.itsmarta.com/train-stations-and-schedules.aspx.

Nessen, S., 2020. New York City's Subway Ends 24-Hour Service Amid Pandemic, National Public Radio,

OpenStreetMap, 2020. Planet dump retrieved from https://planet.osm.org. https://www.openstreetmap.org.

Pinto, H.K.R.F., Hyland, M.F., Mahmassani, H.S., Verbas, I.O., 2020. Joint design of multimodal transit networks and shared autonomous mobility fleets. Transp. Res. C 113, 2-20. http://dx.doi.org/10.1016/j.trc.2019.06.010.

Reed, T., 2019. Global Traffic Scorecard. INRIX.

Riley, C., Legrain, A., Van Hentenryck, P., 2019. Column generation for real-time ride-sharing operations. In: Rousseau, L.-M., Stergiou, K. (Eds.), Integration of Constraint Programming, Artificial Intelligence, and Operations Research. Springer, pp. 472–487. http://dx.doi.org/10.1007/978-3-030-19212-9_31.

Salazar, M., Rossi, F., Schiffer, M., Onder, C.H., Pavone, M., 2018. On the interaction between autonomous mobility-on-demand and public transportation systems. In: 2018 21st International Conference on Intelligent Transportation Systems (ITSC). pp. 2262–2269. http://dx.doi.org/10.1109/itsc.2018.8569381.

Socially Aware Mobility Lab, 2020. How on-demand multimodal transit works. https://sam.isye.gatech.edu/videos.

Tirachini, A., Cats, O., 2020. COVID-19 and public transportation: Current assessment, prospects, and research needs. J. Public Transp. 22 (1), http://dx.doi.org/10.5038/2375-0901.22.1.1.

U.S. Census Bureau, 2020. Means of Transportation to Work by Selected Characteristics. 2015-2019 American Community Survey 5-year estimates.

Van Hentenryck, P., 2019. On-demand mobility systems can ease commuters' burdens – socially aware transit solutions focus on solving 'first/last mile' challenge. ISE Mag. 51 (10), 28–33.

Wickert, D., 2020a. MARTA Bus Cuts Have Many Riders Scrambling to Find a Ride. The Atlanta Journal-Constitution.

Wickert, D., 2020b. MARTA Cuts Most Bus Routes, Beefs Up Others Amid Pandemic. The Atlanta Journal-Constitution.

World Health Organization, 2020. WHO director-general's opening remarks at the media briefing on COVID-19 - 11 March 2020. https://www.who.int/dg/speeches/detail/who-director-general-s-opening-remarks-at-the-media-briefing-on-covid-19---11-march-2020.